Thermal stress and Thermal expansion in a brake drum of heavy commercial truck

By

THAWEESAK HEMCHI

Dissertation submitted in partial fulfillment of
the requirements for the
Bachelor of Engineering (Hons)
(Mechanical Engineering)

JULY 2008

Universiti Teknologi PETRONAS
Bandar Seri Iskandar
31750 Tronoh
Perak Darul Ridzuan

CERTIFICATION OF APPROVAL

Thermal Stress and Thermal Expansion in a brake drum

of heavy commercial truck

by

THAWEESAK HEMCHI

A project dissertation submitted to the
Mechanical Engineering Programme
Universiti Teknologi PETRONAS
in partial fulfilment of the requirement for the
BACHELOR OF ENGINEERING (Hons)
(MECHANICAL ENGINEERING)

Approved by,

_____
(Dr. Khairul Fuad)

UNIVERSITI TEKNOLOGI PETRONAS

TRONOH, PERAK

JULY 2008

CERTIFICATION OF ORIGINALITY

This is to certify that I am responsible for the work submitted in this project, that the original work is my own except as specified in the references and acknowledgements, and that the original work contained herein have not been undertaken or done by unspecified sources or persons.

_____

THAWEESAK HEMCHI

ABSTRACT

Brake system is one of crucial system in automobile. Poor performance or brake failure will cause fatal accident especially for heavy transportation vehicle. Excessive thermal stresses may cause undesirable effects on the material of brake drum that eventually lead to the initiation of a crack. This dissertation investigates the thermal stress and thermal expansion develops in a brake drum of heavy commercial truck due to temperature distribution in severe braking condition. The analysis is done by simulate the temperature distribution and the thermal stress distribution within the drum material using finite element approach in ANSYS simulation program. Before the simulation work, dynamic of moving truck and rotating drum are analyzed. Also, the energy conversion analysis is made to determine amount of frictional heat flux created, which the values will be applied in the simulation input for the temperature distribution. And the temperature distribution result will be applied in the structural analysis field as the input for thermal stress and expansion analysis. The simulation results give the highest temperature of 255˚C at the middle of braking period which is 2.6 second. The maximum thermal stress result is achieved 93 MPa at 1.32 second after braking started and the maximum thermal expansion is achieved in radial expansion of 2.9 millimeter at 2.6 second of braking period. The evaluation of simulation results give the information for prediction and contribute toward improving design, modeling and analysis technique for integrity of thermo-mechanical system that subjected to high temperature.

ACKNOWLEDGEMENT

First and foremost, thank to Allah S.W.T for the strength given to carry out all the tasks allocated for final year project I and II throughout a year.

With the name of Almighty God, the author would like to thank the endless help and support received from project supervisor, Dr Khairul Fuad for his willingness to be the main supervisor for the author. Special thank to him for the efforts in providing the best knowledge and technical expertise for the author. Without his guidance and patience, the author would not be succeeded to complete the project. His guidance and advices are very much appreciated.

The author has furthermore to thank his work colleagues for all their help, ideas and valuable supports throughout the completion of this project.

Finally, heartfelt thanks go to author's beloved family for their endless support and encourage throughout the completion of this project. Thank you.

TABLE OF CONTENTS

LIST OF ILLUSTRATION

FIGURES

TABLES

NOMENCLATURE

σ	Thermal stress (Pa)
E	Modulus of elasticity (Pa)
α_l	Linear coefficient of thermal expansion (m/m˚C)
ΔT	Variation of temperature (˚C)
∂L	Displacement of length (m)
u	Initial truck velocity (m/s)
v	Final Truck velocity (m/s)
a	Truck acceleration (m/s^2)
t	Braking time (s)
s	Braking distance (m)
v_t	Drum tangential velocity (m/s)
a_t	Drum tangential acceleration (m/s^2)
ω	Drum angular velocity (rad/s)
α_d	Drum angular acceleration (rad/s^2)
θ	Drum angular displacement (rad)
Δt	Time interval (s)
D	Tyre outer diameter (m)
d	Drum inner diameter (m)
F	Total force to stop the truck (N)
F_{fr}	Friction force between brake shoe and rubbing surface (N)
ΔU	Work of force to stop the truck (J)
T	Kinetic energy of moving truck (J)
m	Truck-trailer mass (kg)
g	Gravitational acceleration (9.81 m/s^2)
ΔQ	Heat absorbed in time interval (J)
A	Shoe-drum contact area (m^2)
q	Frictional heat flux (W/m^2)
k	Thermal conductivity (W/m.K)
C_p	Specific heat (J/kg.K)
α	Thermal diffusivity (m^2/s)

ρ	Density (kg/m^3)
h	Coefficient convection heat transfer (W/m^2.K)
T	Temperature (˚C)
E	Energy generation (J)
dx	x-axis direction
dy	y-axis direction
dz	z-axis direction
dr	Radial direction
$d\Phi$	Angular direction
p	Time denotation
m	Nodes at horizontal position
n	Nodes at vertical position
Fo	Fourier number
Bi	Biot number
Δx	Distance between nodes

CHAPTER 1

INTRODUCTION

1.1 BACKGROUND OF STUDY

Brake system is the most important system in motorized vehicle. Several safety aspects which are offered by brake system are either to slow, to stop or to hold the vehicle stationary. Inefficient performance of braking system may cause undesirable effects on the vehicle's safety reliability. However, failure in such system might cause fatality especially for large commercial vehicle. With rapid technology development in the road transportation, heavy vehicles like trucks and busses have been suffering an increase in size and load capacity. The development of more efficient brake has become significant with this kind of situations.

Normally, what defines the mechanical properties of the drum and lining is according the temperature created at most severe braking condition. With short braking period from a high speed while carrying a huge load, the maximum heating is generated and the least possibility of the heat absorb to flow out of the system. So, the design must offer the functionality, performance and reliability up to user's expectation as they concern about the driving safety.

The temperature of the brake drum increases during each stop. The amount of increment will be determined by the vehicle speed and weight, the rate of stop and the mass of the brake components, especially that of drum and rotors. If the stop is gradual, from a slow speed and long in duration, the force required to stop is less and the heat generated probably flow away as quick as it is generated and the drum will not get much hotter than the ambient temperature. If the stop is rapid in short period of time, from high speed and the vehicle is heavy, the brake will requires

larger force required to stop and generates more heat than can be easily dissipated and brake components will get very hot.

1.2 SIGNIFICANCE OF STUDY

This project is to study the thermal stress and thermal expansion develops in a brake drum system in order to improving the performance of brake drum and reducing the failure probability. This project contributes to the technical aspects of mechanical thermal design such as:

- Develops a computational approach to predict the transient response of brake drum subjected to high frictional heat flux caused by high speed sliding friction.
- Contributes to the advancement for study on initiation and growth of crack that occurred on drum surface due to excessive thermal stress and thermal expansion.
- Contributes to the advancement of design, modeling, material selection and analysis techniques for temperature distribution such that they can be applied to general mechanical heat transfer problems, not just limited to brake drum.

1.3 PROBLEM STATEMENT

The thermal stress and thermal expansion that occur in a brake drum during braking may cause undesirable effects on the material of the brake drum that eventually lead to the initiation of a crack. These effects are small for a small car, but they can cause trouble for a large commercial vehicle like truck. The predominant trend in the development of large vehicles is to ward higher vehicle speed and heavier loads, which considerably increase the energy required to stop the vehicle, maximum heat created and few amount of heat able to be dissipated by the brake drum.

1.4 OBJECTIVES

The corresponding research objectives are outlined as follows:

- To investigate the thermal stress and thermal expansion in a brake drum of heavy commercial truck in the course of braking.
- To acknowledge the type of material failure in drum and the cause of it.
- To understand the concept of heat generation due to sliding friction and the method of heat transfer in transient temperature distribution.
- To analyze the kinetics and dynamics of truck-trailer and the brake drum associated to the real breaking condition.
- To understand the concept of computational numerical method for finite element analysis provided by ANSYS to applied in solving thermo-mechanical problems.

1.5 SCOPE OF STUDY

A type of leading and trailing shoe brake assembly is considered to be analyzed in this study. The brake drum undergoes heating and cooling during the brake application, which figured as clock mechanism. The transient temperature distribution in the brake drum will be investigated under the most severe braking condition. Brake is hardly applied by driver that allow the truck experiences 0.5-g deceleration while the truck carries maximum loads, travels at high speed of 100 km/h. Although, it assumed that the frictional heat created at the contact region is constant and equal along the surface. The friction coefficient also is considered constant throughout braking period and the contact is perfect such that the pressure distribution is properly distributed along brake lining.

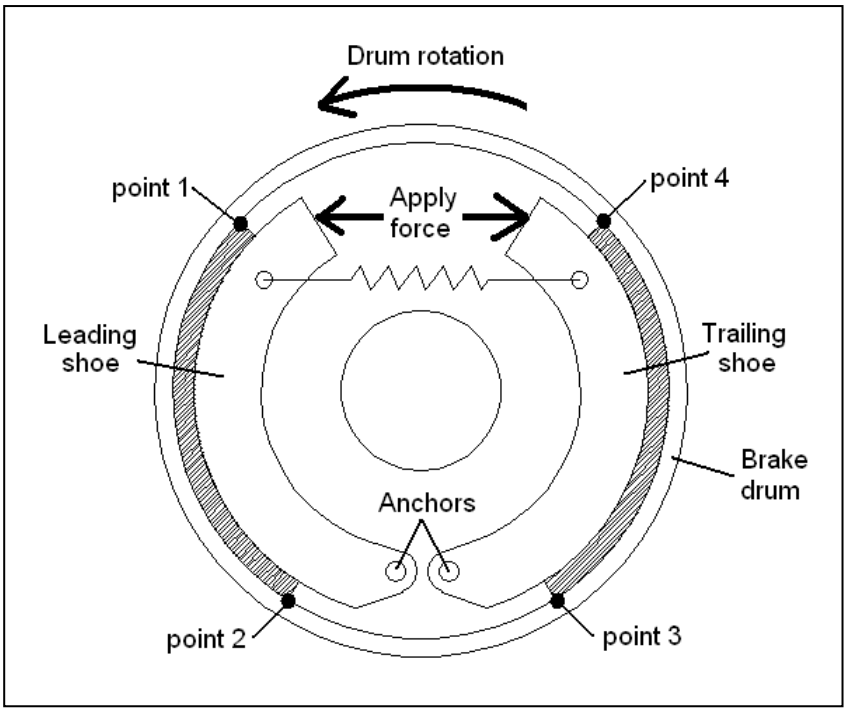

Figure 1.1 The rotation of the brake drum and point set at the brake shoe

In this study, it is considered that the drum absorbs the energy input for the time interval during which the drum moves from one end of the shoe lining to the other end with its varying velocity, say from point 1 to point 2 and point 3 to point 4 in Figure 1.1. Between point 2 and 3 and between point 4 and 1, no more heating is possible while cooling effect through convection will takes place during this period.

Before getting thermal stress and thermal expansion results, the temperature development and distribution are investigated on the drum surface and within the drum body. The maximum temperature achieved at various point is identified and how the temperature is distributed over time. Then, different material is selected with different value of thermal properties to be as a sample on order to investigate the effects on the temperature development and distribution accordance to reference material. All the result obtained will be discussed and the cause will be explained in relation to the theory. Finally, the conclusion is made and recommendation for future study is represented.

CHAPTER 2

LITERATURE REVIEW

2.1 MODELING OF DRUM BRAKE SYSTEM

The procedure to create a linear brake system model includes the following steps: constructing FE models for brake components, performing modal analysis and extracting the modal information (frequencies and mode shapes), adding the effects of lining stiffness and friction forces, and finally incorporating the effects of boundary conditions to form a coupled model.

Four major components participate in the response of a drum brake system: the drum, the brake shoes, the shoe lining, and the backing plate as shown in Figure 2.1. The shoe linings attached on the shoes are in contact with the drum to generate radial as well as friction forces during braking.

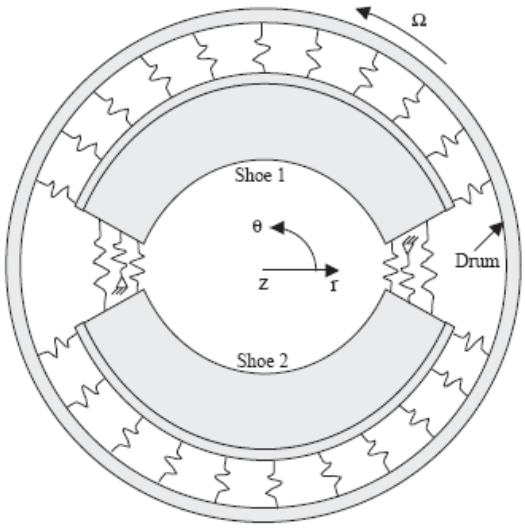

Figure 2.1: Schematic of Drum Brake system

2.2 THERMAL STRESS

Thermal stresses are stresses induced in a body as a result of changes in temperature. An understanding of the origins and nature of thermal stresses is important because these stresses can lead to fracture or undesirable plastic deformation. The two prime sources of thermal stresses are restrained thermal expansion (or contraction) and temperature gradients established during heating or cooling.

When a solid body is heated or cooled, the internal temperature distribution will depend on its size and shape, the thermal conductivity of the material, and the rate of temperature change. Thermal stresses may be established as a result of temperature gradients across a body, which are frequently caused by rapid heating or cooling, in that the outside changes temperature more rapidly than the interior; differential dimensional changes serve to restrain the free expansion or contraction of adjacent volume elements within the piece. For example, upon heating, the exterior of a specimen is hotter and, therefore, will have expanded more than the interior regions. Hence, compressive surface stresses are induced and are balanced by tensile interior stresses. The interior–exterior stress conditions are reversed for rapid cooling such that the surface is put into a state of tension.

The strains are related to the stresses by means of the usual Hooke's law of linear isothermal elasticity. The total strains are the sum of the two components and are therefore related as follows to the stresses and the temperature in any coordinate system.

$$\varepsilon_{xx} = \frac{1}{E}\left[\sigma_{xx} - \nu\left(\sigma_{yy} + \sigma_{zz}\right)\right] + \alpha T$$

$$\varepsilon_{yy} = \frac{1}{E}\left[\sigma_{yy} - \nu\left(\sigma_{zz} + \sigma_{xx}\right)\right] + \alpha T$$

$$\varepsilon_{zz} = \frac{1}{E}\left[\sigma_{zz} - \nu\left(\sigma_{xx} + \sigma_{yy}\right)\right] + \alpha T \qquad (1)$$

Where E is the modulus of elasticity, ε is strain, ν is the Poisson's ratio and α is the coefficient of thermal expansion.

2.3 THERMAL EXPANSION

Thermal expansion is the tendency of matter to change in volume in response to a change in temperature. When a substance is heated, its constituent particles move around more vigorously and by doing so generally maintain a greater average separation. Materials that contract with an increase in temperature are very uncommon; this effect is limited in size, and only occurs within limited temperature ranges. The degree of expansion divided by the change in temperature is called the material's coefficient of thermal expansion and generally varies with temperature.

The thermal expansion coefficient (α) is a thermodynamic property of a substance. It relates the change in temperature to the change in a material's linear dimensions. It is the fractional change in length per degree of temperature change and has units of reciprocal temperature [$(^\circ C)^{-1}$ or $(^\circ F)^{-1}$].

$$\alpha = \frac{1}{L_0}\frac{\partial L}{\partial T} \tag{2}$$

Where L_0 is the original length, L the new length, and T the temperature

The coefficient of thermal expansion is used in:

- Linear thermal expansion,

$$\frac{\Delta L}{L_0} = \alpha_L \Delta T \tag{3}$$

- Area thermal expansion,

$$\frac{\Delta A}{A_0} = \alpha_A \Delta T \tag{4}$$

- Volumetric thermal expansion,

$$\frac{\Delta V}{V_0} = \alpha_V \Delta T \tag{5}$$

2.4 THERMAL LOADING CRACK

Friction brakes are required to transform large amounts of kinetic energy into heat energy at the contact area between rubbing surface and friction material. The temperature generated at the friction interface is a complex phenomenon, which directly affects the braking performance. The contact friction usually leads to dynamic instabilities and temperature generated at the interface even if steady-state conditions are applied to the system. When instabilities are generated, the variables at the contact interface such as thermal stress and velocities can differ than those obtained under steady-state conditions. Therefore, it is necessary to study both dynamic and thermal behavior of the contact in order to understand the phenomena involved during sliding with friction in brake system. As the sliding speed increase, the temperature on rubbing surface will rise. The determination of the temperature field on the sliding surface is a complex problem by the high thermal gradient at the interface.

In the design of engineering components for high temperature applications, heat flux loading is one of potential concern. Under thermal loading cracks and delimitations are discontinuities in the temperature field, impede heat flow and subsequently redistribute temperature. Thermal cracking is commonly observed in truck drum brake with high-g braking condition while carrying extra load on trailer. The cracks fall into 2 broad categories, which are a series of heat cracks that partially penetrate the rubbing surface of drum and thru-cracks that completely pass through the drum wall. Though it is well known that thermal cracks do arise from hard braking, there is no formal treatment of the problem of thru-cracks.

2.5 DRUM MATERIAL FAILURE

There are several conditions that may lead to material failure that occur due to excessive thermal loading. The conditions all are illustrated in Appendix A and explained as following:

- Thru-crack is a crack extending through the entire wall. This condition is caused by excessive heating and cooling of the brake drum during operation.
- Heat-checking is the appearance of numerous short, fine, hairline cracks on the braking surface of the drum. Heat-checking is caused by the constant heating and cooling of the braking surface. It can progress over time into cracks in the braking surface depending on such factors as lining wear rate, brake system balance, and how hard the brakes are used.
- Martensite spotted can be indicated by hard, slightly raised dark colored spots on the braking surface with uneven wear. This condition indicates that the drum has been subjected to extremely high temperature caused by improperly balanced pressure distribution, dragging brake or continued severe brake applications. These extremely high temperatures have caused structural changes to occur in the drum material which makes the drum more susceptible to cracking.
- There is condition called ‘blue drum’ which the sign of bluing has been subjected to extremely high temperatures. This condition may be caused by continued hard stops, by brake system imbalance or improperly functioning return springs. If this bluing is continued over time, it can result in the development of martensite condition or cause the drum to crack.
- Excessive wear normally occurs along the edges of the lining contact area of braking surface. The most common cause of this problem is the build-up of abrasive material from either the presence or absence of dust shields depending on the application of the vehicle.
- Radial cracking of the mount surface is caused by interference between the hub and drum mounting surface during installation as a result of using the wrong drum for the application or improperly cleaning the hub piloting surface prior to drum installation.

2.6 KINETICS AND DYNAMICS PROBLEM

2.6.1 Equation of Rigid Body in Rectilinear Motion

Considering the truck is moved at initial speed of the u, and reached final speed of v after braking. Uniform force is applied on the brake so that the truck is slowed down at constant deceleration, a. the relationship of velocity and acceleration of the truck in linear motion can be defined as

$$v = u + at \tag{6}$$

$$\text{or} \quad v^2 = u^2 + 2as \tag{7}$$

Where t is the time and s is the distance. From this equation, the time taken for initial velocity to final velocity can be determined. Also, the distance traveled by the truck. For this case, the truck is finally stopped after braking where the final velocity becomes zero.

2.6.2 Equation of Rigid Body Motion about a Fixed Axis

The brake drum is rotating about a fixed axis which at the center of the drum diameter. The shoe is move from one edge, point 1 to another edge, point 2 as illustrated in Figure 2.3 and this movement is continues until the truck is fully stopped. Assuming the tangent velocity, v_t at outer point of truck tyre is equal to truck speed and the truck deceleration is also equal to tangent deceleration, a_t of that point. Then, the initial angular velocity, ω and the constant angular deceleration, α of the drum can be determined using equations below:

$$v_t = \frac{1}{2} D\omega \tag{8}$$

$$a_t = \frac{1}{2} D\alpha \tag{9}$$

During braking, the angular velocity will be decrease at constant angular deceleration as the shoe move from point to point. The angular velocity of drum at next point is defined as

$$\omega_1^2 = \omega_0^2 + 2\alpha\theta \tag{10}$$

Where, θ is the angular displacement. In the analysis, the angular displacement is the shoe angle. The time interval of each shoe movement is determine in following equation

$$\omega_2 = \omega_1 + \alpha\Delta t \tag{11}$$

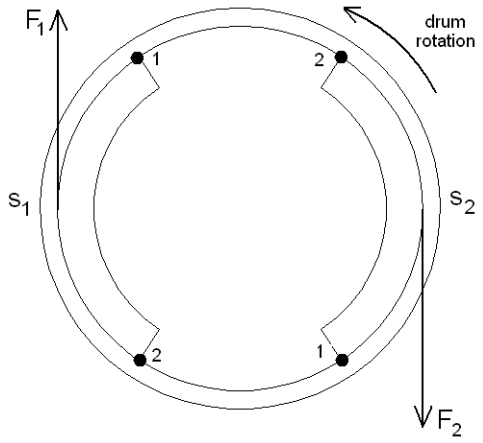

Legend

F_1: Frictional force acting on shoe 1 — s_1: shoe 1 displacement

F_2: Frictional force acting on shoe 2 — s_2: shoe 2 displacement

Figure 2.2: Free-body diagram of drum-show during braking

2.7 WORK AND ENERGY PROBLEM

In mechanics a force F does work on a particle only when the particle under goes a displacement. Same situation happen to the moving truck, force is required in order to stop the truck. The force may constant and in opposite direction of truck movement because the truck is decelerates in constant rate until it is fully stopped. Therefore, the work of force in linear horizontal direction is defined as

$$\Delta U = Fs \tag{12}$$

There is kinetic energy stored within the truck as it is moving. The term kinetic energy is moving particle is defined in form

$$T = \frac{1}{2}mv^2 \tag{13}$$

This term is always in positive scalar. Theoretically, the particle's initial kinetic energy plus the work done by all forces acting on the particle as it moves from its initial to its final position is equal to the particle's final kinetic energy in the form of:

$$T_1 + \Sigma U_{1\text{-}2} = T_2 \tag{14}$$

Final kinetic energy of truck is zero since the final velocity of truck is zero where the truck is fully stopped and the equation is simplified to

$$T = -\Delta U$$

$$or \quad \frac{1}{2}mv^2 = -Fs \tag{15}$$

where m is the total mass of the truck with its trailer load. Negative force indicates that it is acting on opposite direction of truck movement.

Assume that the value of force required to stop the truck is equal to total frictional force subjected to the all drum rubbing surfaces. Also, assume that the brake force distribution is 60% at front, 20% at rear and 20% at back-trailer. Highest force is applied on front brake drum and the amount of frictional force acting on one of them is as below

$$F_{fr} = 0.3F \tag{16}$$

Since there is force acting at one point and it is moving in certain distance, work is done that caused by sliding friction. Assume that the heat energy created is equal to work of friction and only 95% of heat energy is absorb by the drum. So, the heat energy absorbed due to friction from point 1 to 2 is

$$\Delta Q = 0.95 F_{fr} s_{1-2} \tag{17}$$

Then, heat flux applied on one shoe can be expressed as

$$q_{1-2} = \frac{1}{2}\left(\frac{\Delta Q}{\Delta t A}\right) \tag{18}$$

2.8 ANALYSIS OF TEMPERATURE DISTRIBUTION

A major objective in a conduction analysis is to determine the temperature field in a medium. That is, it is wished to know the temperature distribution, which represents how temperature varies with position in the medium. One this distribution is known, the conduction heat flux at any point in the medium or on its surface may be computed from Fourier's Law.

2.8.1 Cartesian Coordinates

Consider a homogeneous medium within which there is no bulk motion (advection) and the temperature distribution $T(x,y,z)$ is expressed in Cartesian coordinates. If there are temperature gradients, conduction heat transfer will occur across each of the control surfaces as shown in Figure 2.3. The conduction heat rates at the opposite surfaces can then be expressed as a Taylor series expansion where,

$$q_{x+dx} = q_x + \frac{\partial q_y}{\partial x} dx \tag{19.a}$$

$$q_{y+dy} = q_y + \frac{\partial q_y}{\partial y} dy \tag{19.b}$$

$$q_{z+dz} = q_z + \frac{\partial q_z}{\partial x} dx \tag{19.c}$$

In words, Eq. (19) simply states that the x component of the heat transfer rate at x+dx is equal to the value of this component at x plus the amount by which it

changes with respect to x time to *dx*. Within the medium, there may also be energy generation term represented by

$$\dot{E} = \dot{q}\, dxdydz \tag{20}$$

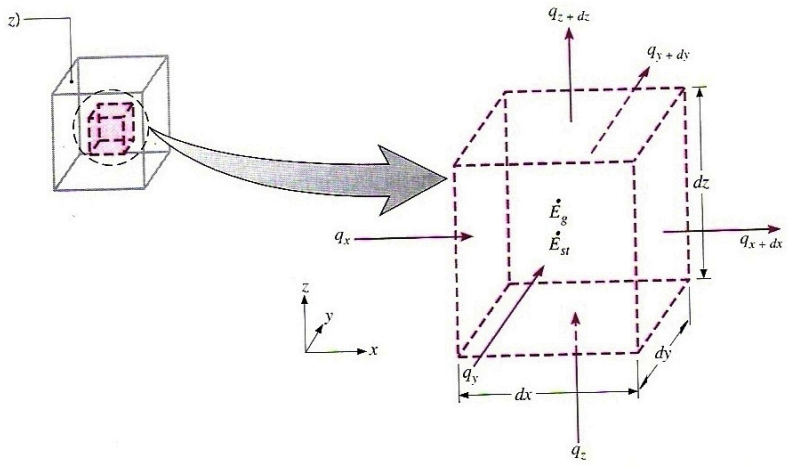

Figure 2.3: Differential control volume for conduction analysis in Cartesian Coordinates

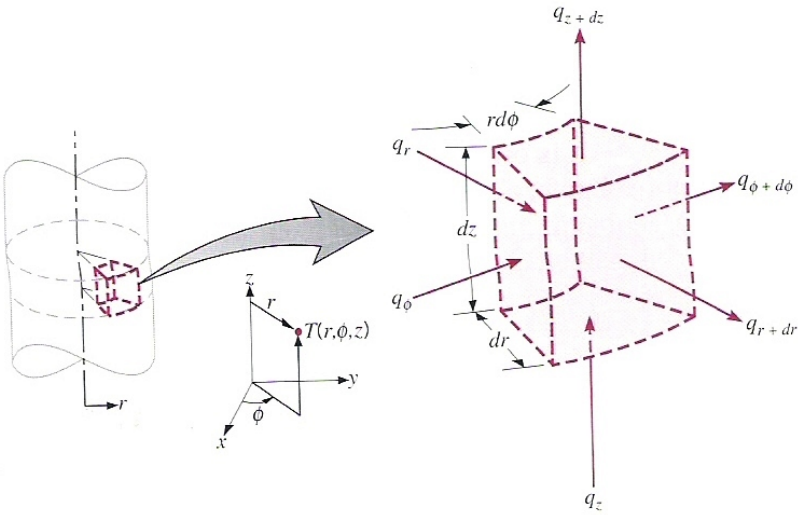

Figure 2.4: Differential control volume for conduction analysis in Cylindrical coordinates

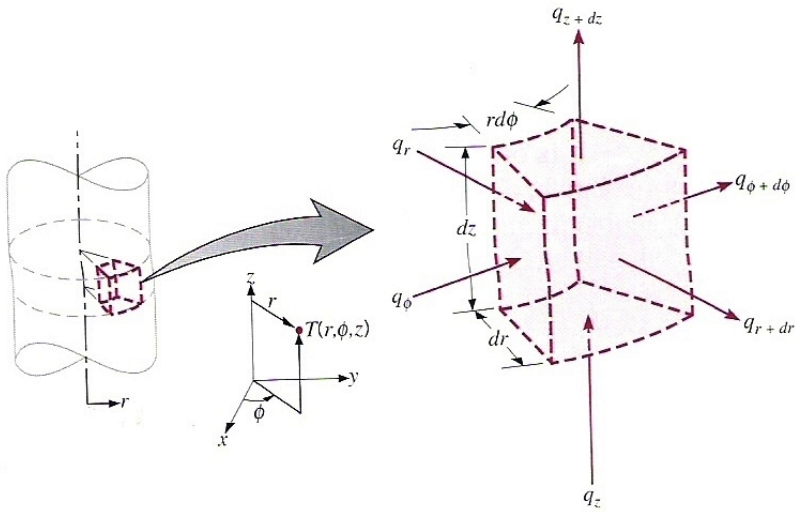

Figure 2.5: Differential control volume for conduction analysis in Spherical coordinates

In addition, there changes may occur in amount of internal thermal energy stored. If the material not experiencing phase change, latent energy effects are not pertinent, then energy storage term expressed by

$$\dot{E} = \rho c_p \frac{\partial T}{\partial t} dxdydz \tag{21}$$

On the rate basis, the general form of conservation of energy requirement is

$$\dot{E}_{in} + \dot{E}_g - \dot{E}_{out} = \dot{E}_{st} \tag{22}$$

Substituting all Eq. (19), Eq. (20) and Eq. (21) into Eq. (22),

$$-\frac{\partial q_x}{\partial x} dx - \frac{\partial q_y}{\partial y} dy - \frac{\partial q_z}{\partial z} dz + \dot{q}\, dxdydz = \rho c_p \frac{\partial T}{\partial t} dxdydz \tag{23}$$

Evaluating from Fourier's Law, the final equation is formed

$$\frac{\partial}{\partial x}\left(k\frac{\partial T}{\partial t}\right) + \frac{\partial}{\partial y}\left(k\frac{\partial T}{\partial t}\right) + \frac{\partial}{\partial z}\left(k\frac{\partial T}{\partial t}\right) + \dot{q} = \rho c_p \frac{\partial T}{\partial t} \tag{24}$$

Eq. (24) is the general form, in Cartesian coordinates, of heat diffusion equation. This equation provides a basic tool for heat conduction analysis. From its solution,

the temperature distribution $T(x,y,z)$ as a function of time can be obtained. In word, it states that at any point in the medium the rate of energy transfer by conduction into a unit volume plus the volumetric rate of thermal energy generation must equal the rate of change of thermal energy stored within the volume.

2.8.2 Cylindrical Coordinates

The general form of the heat flux vector of Fourier's Law in cylindrical coordinates expressed as

$$q'' = -k\nabla T = -k\left(i\frac{\partial T}{\partial r} + j\frac{\partial T}{\partial \phi} + k\frac{\partial T}{\partial z} \right) \tag{25}$$

Applying an energy balance to the differential control volume in Figure 2.4, the following general form heat equation is obtained

$$\frac{1}{r}\frac{\partial}{\partial r}\left(kr\frac{\partial T}{\partial r} \right) + \frac{1}{r^2}\frac{\partial}{\partial \phi}\left(k\frac{\partial T}{\partial \phi} \right) + \frac{\partial}{\partial z}\left(k\frac{\partial T}{\partial z} \right) + \dot{q} = \rho c_p \frac{\partial T}{\partial t} \tag{26}$$

2.8.3 Spherical Coordinates

The general form of the heat flux vector and Fourier' Law in spherical coordinates is

$$q'' = -k\nabla T = -k\left(i\frac{\partial T}{\partial r} + j\frac{1}{r}\frac{\partial T}{\partial \theta} + k\frac{1}{r.\sin\theta}\frac{\partial T}{\partial \phi} \right) \tag{27}$$

Applying an energy balance to the differential control volume of Figure 2.5, the following general form of heat equation is obtained

$$\frac{1}{r^2}\frac{\partial}{\partial r}\left(kr^2\frac{\partial T}{\partial r} \right) + \frac{1}{r^2\sin^2\theta}\frac{\partial}{\partial \phi}\left(k\frac{\partial T}{\partial \phi} \right) + \frac{1}{r^2\sin\theta}\frac{\partial}{\partial \theta}\left(k.\sin\theta\frac{\partial T}{\partial \theta} \right) + \dot{q} = \rho.c_p\frac{\partial T}{\partial t} \tag{28}$$

2.9 COUPLE-FIELD ANALYSIS

A coupled-field analysis is an analysis that takes into account the interaction (coupling) between two or more disciplines (fields) of engineering. An example of this type of analysis is a sequential thermal-stress analysis where nodal temperatures from the thermal analysis are applied as "body force" loads in the subsequent stress analysis. The physics analysis is based on a single finite element mesh across physics. Physics files can be used to perform coupled-field analysis. Physics files are created which prepare the single mesh for a given physics simulation. A solution proceeds in a sequential manner. A physics file is read to configure the database, a solution is performed, another physics field is read into the database, coupled-field loads are transferred, and the second physics is solved. Coupling occurs by issuing commands to read the coupled load terms from one physic to another across a node-node similar mesh interface.

2.9.1 Sequentially Coupled Physics Analysis

A sequentially coupled physics analysis is the combination of analyses from different engineering disciplines which interact to solve a global engineering problem. The term sequentially coupled physics refers to solving one physics simulation after another. Results from one analysis become loads for the next analysis. If the analyses are fully coupled, results of the second analysis will change some input to the first analysis.

The ANSYS program performs sequentially coupled physics analyses using the concept of a physics environment. The term physics environment applies to both a file you create which contains all operating parameters and characteristics for a particular physics analysis and to the file's contents which is the thermal result file to be input in the next structural analysis.

2.10 FINITE ELEMENT METHOD

Finite element methods have been developed to a high level of refinement in structural mechanics. Such methods are also applicable to steady and transient heat transfer problems and are being used extensively to model and simulate a wide variety of practical and fundamental problems.

Finite element methods provide piecewise, or regional, approximations to partial differential equations. Finite difference methods generally provide point-wise approximations. Finite difference methods are relatively easy to implement, except when irregular geometries or unusual boundary conditions are present. Under such conditions, it may be desirable to use a more general approach, such as finite element method, even at the expense of programming complexity.

A finite element is a discrete spatial region that is a subdivision of a continuum. A finite element method (FEM) is a mathematical procedure for satisfying a partial differential equation in an average sense over a finite element. Various methods exist. All of them require that an integral representation of a partial differential equation be constructed. Classical finite element methods for structural mechanics are based on variation principles. Variation principles also apply to steady-state diffusion and conduction processes. However, for transient diffusion and conduction and for convective transfer processes, it is necessary to use more general procedures, such as a method of weighted residuals.

The solution of a physical problem by a finite element method follows a well-defined sequential process. First, the physical region is discredited into elements. The number, type and allocation of elements are often a matter of judgment. Second, interpolation or shape functions are selected for the elements. The interpolation functions represent the assumed form of spatial solution in the elements and are related to the number of nodes in the elements. Third, the matrix equations for an individual element are formulated using integral statement for the element as a guide. Fourth, the matrix equations for the overall system, consisting of all elements are assembled. Finally, global equations that are of the same form as the element equations but are of larger dimension are solved.

2.10.1 Finite Element Solution

A finite element formulation is often appropriate for multidimensional conduction, especially when the geometric boundaries of the conducting region are irregular and are not aligned with a natural coordinate system. In such cases any extra effort in setting up a finite element solution may be more than offset by the ease which the boundary regions can be handled.

In general, the finite element approaches proceeds in a stepwise fashion. The first step is to discretize the conducting region into finite elements, and to choose an appropriate interpolation procedure for use within the elements. The next step is to use the appropriate integral statement for the problem. The appropriate integral statement for a Galerkin finite element approach is

$$\int (\nabla p_i).(k\nabla T)dV = \int_V p_i \dot{Q} dV - \int_{S1+S2+S3} p_i . q_n dS \tag{29}$$

Where N is the number of nodal points in the system and i = 1, 2,…, N. The shape function p_i appears as the weighting function, V denotes the heat conducting volume, and S_1, S_2 and S_3 denote external boundaries of the system corresponding to prescribed temperature (S_1), prescribed flux (S_2) and a convective heat transfer coefficient (S_3), respectively.

To apply the integral statement, it is necessary to replace the unknown temperature T in Eq. (29) by approximation function $\widetilde{T}$. The latter is given in terms of the shape function p_i and the nodal values of temperature T_i by

$$T(\bar{x}) \approx \widetilde{T}(\bar{x}) = \sum_{i=1}^{N} p_i(\bar{x}) T_i \tag{30}$$

After substituting Eq. (30) into Eq. (29), the matrix equation as follow is obtained

$$(A^*)(T) = (F^*) \tag{31}$$

or $$(A_K)(T) = (F_Q) + (F_{S1}) + (F_{S2}) + (F_{S3}) + (A_{S3})(T) \tag{32}$$

For Cartesian coordinates, the elements of the matrices and vectors in Eq. (32) are given for three-dimensional diffusion as

$$
\begin{aligned}
\left(A_K\right)_{i,j} &= \int_V k\left(\frac{\partial p_i}{\partial x}\frac{\partial p_j}{\partial x}+\frac{\partial p_i}{\partial y}\frac{\partial p_j}{\partial y}+\frac{\partial p_i}{\partial z}\frac{\partial p_j}{\partial z}\right)dV \\
\left(F_Q\right)_i &= \int_V p_i Q dV \\
\left(F_{S1}\right)_i &= -\int_{S1} p_i q_n dS \\
\left(F_{S2}\right)_i &= -\int_{S2} p_i q_n dS \\
\left(F_{S3}\right)_i &= \int_{S3} p_i h T_f dS \\
\left(A_{S3}\right)_{i,j} &= -\int_{S3} p_i\left(h p_j\right)dS
\end{aligned}
\tag{33}
$$

where i and j are indices ranging from 1 to N. Eq. (32) and Eq. (33) represent the global equations. They also represent the element equations when the range of i and j is restricted to the number of nodal points in an element.

Generally, the matrix system is given Eq. (31) is assembled in an element-by-element fashion. That is the integral statement, Eq. (29) is applied to each element, and the results are added to the global equation as soon as they are available. The most common procedures used for solution are Gaussian elimination and iterative methods. These procedures are similar to those described earlier for finite difference methods. For the iterative methods, the iterating equation is usually found by solving the individual equation in Eq. (31) for term on the diagonal. Before starting a solution it is necessary to condense the vector of unknowns (T). In particular, the equations corresponding to boundary nodes with Dirichlet conditions (prescribed temperature) must be removed.

2.10.2 Practical Implementation

Different approaches can be used to generate, assemble and solve governing system of algebraic equations. The results obtained are stored and processed using interpolation functions to obtain the desired field variables and relevant derived quantities in the form of graphs, tables, and correlating equations.

While the preceding aspects give rise to considerable flexibility and versatility in FEM solutions, they also make it desirable to use available software, whenever possible, to simplify code development for the practical implementation of the method. A typical finite element program consists of the following 3 main parts:

1. *Preprocessor*. In this portion of the computer program, the input data, pertaining to the geometry and dimensions of the computational domain, boundary conditions, governing differential equations, and finite element mesh, are read. The type, number, dimensions and coordinates of the elements are read or generated. Information on the interpolation and weighting functions is also read or generated. The input data may be printed and the mesh plotted to show coverage of the computational region.
2. *Processor*. This is main, or central, portion of the program. Here, the element coefficient matrices and column vectors are determined. The boundary conditions are numerically imposed. The element equations are assembled. The system of algebraic equations is solved to yield the values of the various field variables such as temperature, pressure and concentration at the nodes.
3. *Postprocessor*. Once the field variables are obtained at the nodes, the results at points other than the nodes are computed by using interpolation function and the available value at the nodes. Derived variables and quantities, such as stream function, heat transfer rate, heat transfer coefficient, as needed, are obtained from the calculated variables. The output data are then processed to present the results in desired format like graphs and contour plots.

2.10.3 Finite Element in ANSYS

SOLID90 is a twenty-node brick element used to model steady-state or transient conduction heat transfer problems. Each node of the element has a single degree of freedom-temperature-as shown in Figure 2.6. This element is well suited to model problems with curved boundaries. The required input data and the solution output are similar to the data format of the SOLID70 elements.

The 20-node thermal element is applicable to a 3-D, steady-state or transient thermal analysis. If the model containing this element is also to be analyzed structurally, the element should be replaced by the equivalent structural element such as SOLID95. For heat transfer problems, the spatial variation of the temperature over an element is given by:

$$T = \frac{1}{8}\left[T_I(1-s)(1-t)(1-r)(-s-t-r-2) + T_J(1+s)(1-t)(1-r)(s-t-r-2)\right]$$
$$+\frac{1}{8}\left[T_K(1+s)(1+t)(1-r)(s+t-r-2) + T_L(1-s)(1+t)(1-r)(-s+t-r-2)\right]$$
$$+\frac{1}{8}\left[T_M(1-s)(1-t)(1+r)(-s-t+r-2) + T_N(1+s)(1-t)(1+r)(s-t+r-2)\right]$$
$$+\frac{1}{8}\left[T_O(1+s)(1+t)(1+r)(s+t+r-2) + T_P(1-s)(1+t)(1+r)(-s+t+r-2)\right] \quad (28)$$

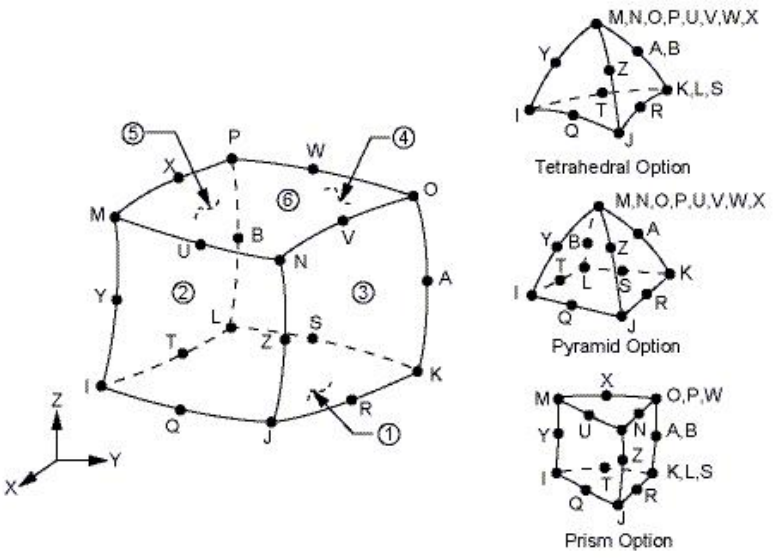

Figure 2.6: The SOLID90 element used in ANSYS

CHAPTER 3

METHODOLOGY

3.1 PROJECT FLOW

The flowchart of the main activities is shown in Figure 3.1.

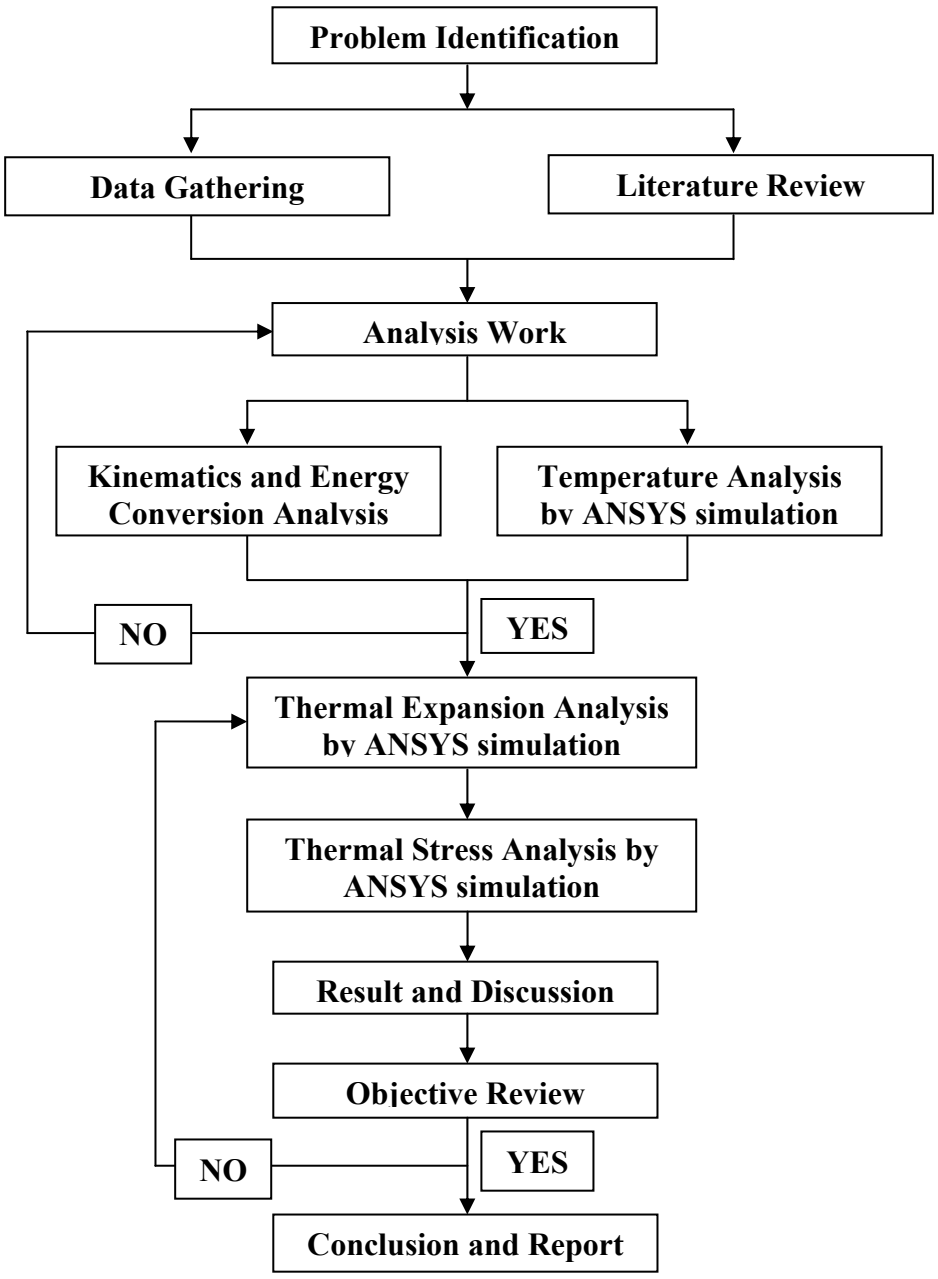

Figure 3.1: Overall project flow of the study

3.2 DATA GATHERING

The actual drum dimension and truck specification is required in order to ensure result of temperature distribution is approximate to real condition. In order to seek required information and data, the truck and trailer builder is searched in order to measured real brake drum dimension. The maximum allowable load for the trailer is identified. All data available for this truck and drum are listed in Table 1. In addition, the dimension of sample drum also is attached in Appendix B.

Table 1: Data available obtained from real truck and drum

Parameter	Value
Truck and tailor weight, m	40000 kg
Truck tyre diameter, D	0.981 m
Drum inner diameter, d	0.42 m
Shoes contact angle, θ	100 degree
Shoe width, W	0.20 m

A specific drum material is selected, also as the reference material for this analysis that is Gray Iron A48 Class 40. The thermal properties of the material are as table below:

Table 2: Thermal properties for Gray Iron A48 Class 40

Parameter	Value
Thermal conductivity, k	55 W/m.k
Specific heat, C_p	550 J/kg.K
Density, ρ	7196 kg m^3
Thermal diffusivity, α	12.89 x 10^{-6} m^2/s
Coefficient of convection	51 W/m^2.K
Coefficient of thermal expansion, α_l	11.4 x 10^{-6} $^{\circ}C^{-1}$
Melting point, T	1120 ˚C

3.3 SIMULATION INPUT CALCULATION

The kinematics movement of the drum during braking is analyzed to identify several important subjects such as total time taken to stop, total distance taken to stop, total shoe movement, angular deceleration, angular velocity, time interval of each shoe movement, heat flux and total heat energy absorbed by drum. The calculation of each subject is performed at each shoe movement, which is from one edge to another edge with displacement of 100 degree. Several assumptions are made to perform the calculation:

- Drum is in stationary while the shoe is rotating in counter-clockwise direction
- Brake distribution is 60% on front, 20% on rear and 20% on trailer
- Force distributed on one brake drum in is equal the total frictional force applied on rubbing surface and
- Kinetics energy is 100% converted to heat energy and only 95% of heat is absorbed by the drum and the rest 5% is absorbed by shoe.

In calculation procedures, first of all the total braking time and distance taken to stop the truck is identified from Eq. (6) and Eq. (7) respectively. From it, the value of angular deceleration is obtained from Eq. (9) and then, the shoe angular velocity for each instantaneous movement is calculated using Eq. (10) by knowing the constant angular deceleration and angular displacement. Next, the time interval of each movement is determined in Eq. (11). The total force required to stop the truck is determined through Eq. (15). Then, the maximum frictional force exerted on rubbing surface is calculated using Eq. (16) and from that amount of heat energy absorbed by drum at that particular time is calculated using Eq. (17). Finally, the amount of heat flux applied for each shoe movement is obtained by computed it using Eq. (19).

The value of heat flux and accumulative time interval of each shoe movement obtained will be as an input in ANSYS solution. All of the calculation is automatically done by Microsoft Excel by programming particular equation.

3.4 DRUM MODELING

The three-dimensional drum is modeled in ANSYS environment in accordance to actual dimension obtained by measuring the actual brake. First of all, the two-dimensional brake cross-sectional profile is drawn and area is created within the combination of lines. For Case 1, the profile is included with circumferential reinforcement while Case 2 is not included. Then, this area is revolved about a fixed axis which is located at center of the brake drum.

The brake volume is divided to 18 sections which created 20^{o} surface angle for each section. Each shoe will make contact at surface angle of 100^{o} each and leave rest surface of two 80^{o} which not make any contact to shoe. One contact surface is selected from 5 sections as illustrated in Figure 3.2. For each time step, this contact section will move at distance of 1 section and continues until 18^{th} section to form a complete rotation. Heat flux will be applied on contact section surfaces and convection load is applied on remaining surface.

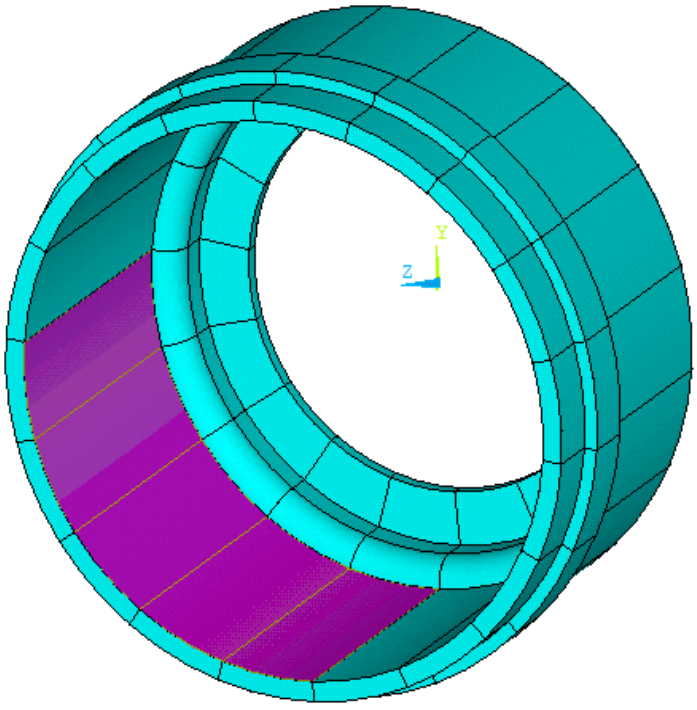

Figure 3.2: Section highlighted represent shoe contact area where heat flux is applied

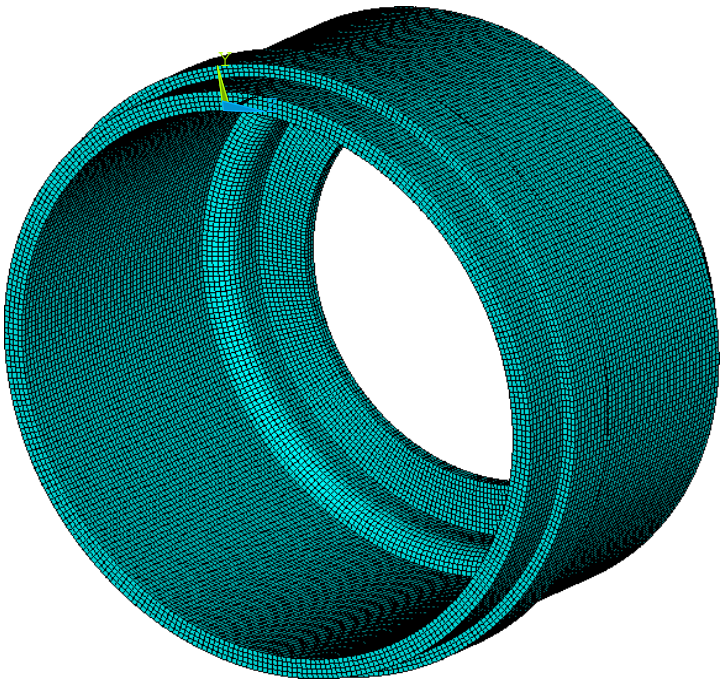

(a)

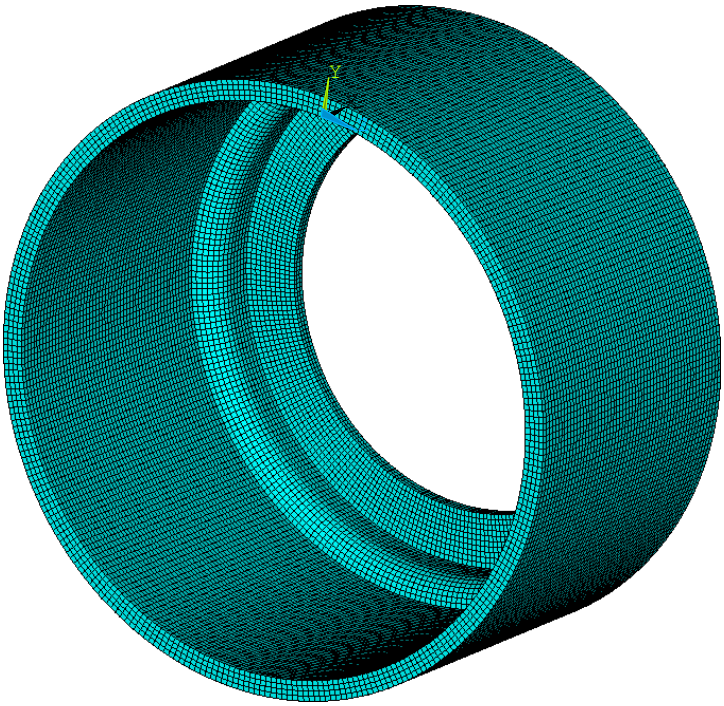

(b)

Figure 3.3: Drum meshing three-dimensional models for (a) Case 1 and (b) Case 2

SOLID90 is chosen as the element type since the simulation is done in three-dimensional model and temperature is the only degree of freedom. Then, both models are meshed by using wedged hexahedral element shape. Appropriate element length is identified using try and error method until it produces best and most consistent element shape. This process is important since the mesh pattern significantly contribute to the accuracy of the simulation result. . It is finally come out with length element of 0.004 m and this value give best mesh for the model volume. There are total of 47736 and 43166 elements in Case 1 and Case 2 model, respectively. The complete drum model is shown in Figure 3.3.

3.5 SIMULATION SOLVING

After the model is completed, the material properties are defined. Full transient analysis is selected with the initial drum temperature of 30^{o}C. In applying the thermal load to the model, it is assumed that:

- Thermal properties are invariant with temperature
- Coefficient of friction remains constant during braking
- Heat flux applied is constant along the contact surface
- Film coefficient of convection is remains constant at all time.

A different amount of heat flux and surface location is applied for each shoe movement. In order to simulate different thermal value and applied area, load step definition is used which represent the shoe movement. Each load step will be solved subsequently without resetting the previous result. In other word, once a load step is solves, ANSYS will continue solves next load step by refers to previous result as initial condition and applies the load in current load step. For each load step, the value of heat flux is taken from the result of kinematics and energy calculation performed in Microsoft Excel. However, the applied areas are determined by reselecting the contact surface for current shoe position. This step is repeated until total 92 of 100 degree shoe movement when the drum angular velocity is reached zero.

For each load step, time step needed to be set. The time step will limit the solution time in time interval defined for each shoe movement. Since ANSYS used explicit to implicit solution, appropriate time step should be calculated for stability criterion. The best limitation time step for this simulation is selected to 0.30 second. So if the time interval is greater than time step, the solving process will be divided into several steps so that the time is maintained less than it is allowed.

Initially, each load step is defined manually by clicking on the Graphic User Interface (GUI) in ANSYS. Somehow, this method consumes very long time since there are 92 load steps need to be defined and saved. In case of mistake, error or changes in value occurred, every single load step need to redefine and this is really waste significant amount of time. So, an alternative is taken by defining the load step using ANSYS command language since modification is easier to be done in text form. Each command written is defining heat flux at selected areas, apply the convection at cooling surface and set the time interval for each load. They are created in notepad and will be read as an input in ANSYS. The example of command to define one load step is shown in Appendix F. Although, writing same 92 commands also consuming time.

Then, the writing command process is done by program it using Borland C++. In the programming, code of loop is used so that the written command is repeated and stops at desired number of repetition that is 92. Also, coding also is created to perform the calculation of heat flux, time and contact areas which are varied from one load step to another. All the programming output will be come out as a text file in notepad and can be directly read into ANSYS input. The sample C++ program code is attached in Appendix F.

After get all the temperature develop in a brake drum result. The results are now written in the thermal result file (*.rth). This file will be the input result file in the structural analysis in order to get the thermal stress and thermal expansion analysis results. Before solving, the structural material properties and the fixed points have been defined. In the solving progress, it also will repeat the same load steps which are 92 load steps. Somehow, this method also consumes very long time since there

are 92 load steps need to be defined and saved. So, an alternative is taken by defining the load step using ANSYS command language since modification is easier to be done in text form. Each command written is defining the drum temperature at selected times. They are created in notepad for by Boland C++ program and will be read as an input in ANSYS. The example of command to define one load step is shown in Appendix G.

3.6 OBTAINING THE SIMULATION RESULT

After the simulation is done, the result of temperature development and distribution is observed. There are 2 ways of observing the result, which are read it on drum surface and inside the drum volume. For temperature on drum surface, the value can be directly obtained from the 3D model. However, for temperature inside drum volume, the drum is cut-cross to expose the inner side as shown in Figure 3.4. The cut section is illustrated in Figure 3.5. All the required result data obtained is tabulated and necessary graphs are plotted.

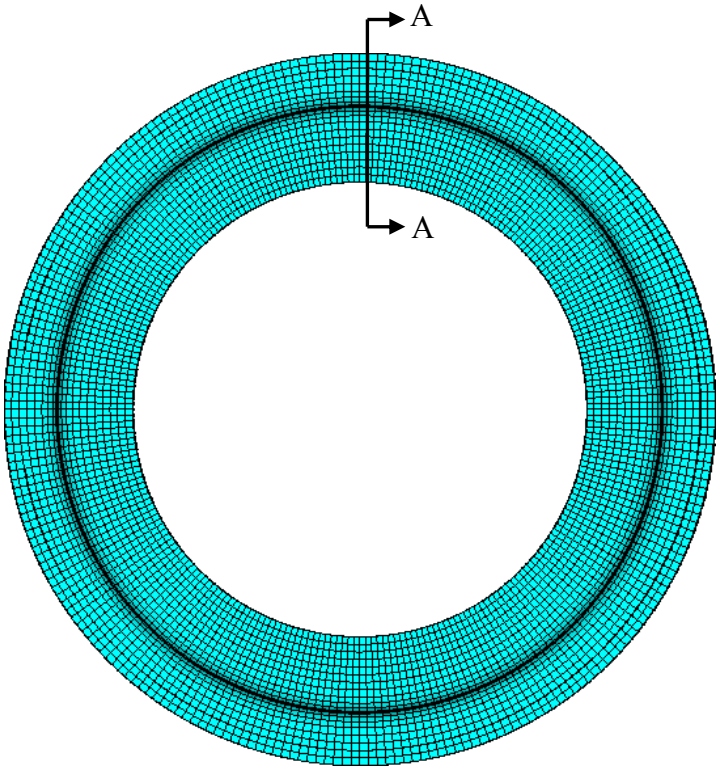

Figure 3.4: The front view of 3D model and section A-A represent the cutting plane

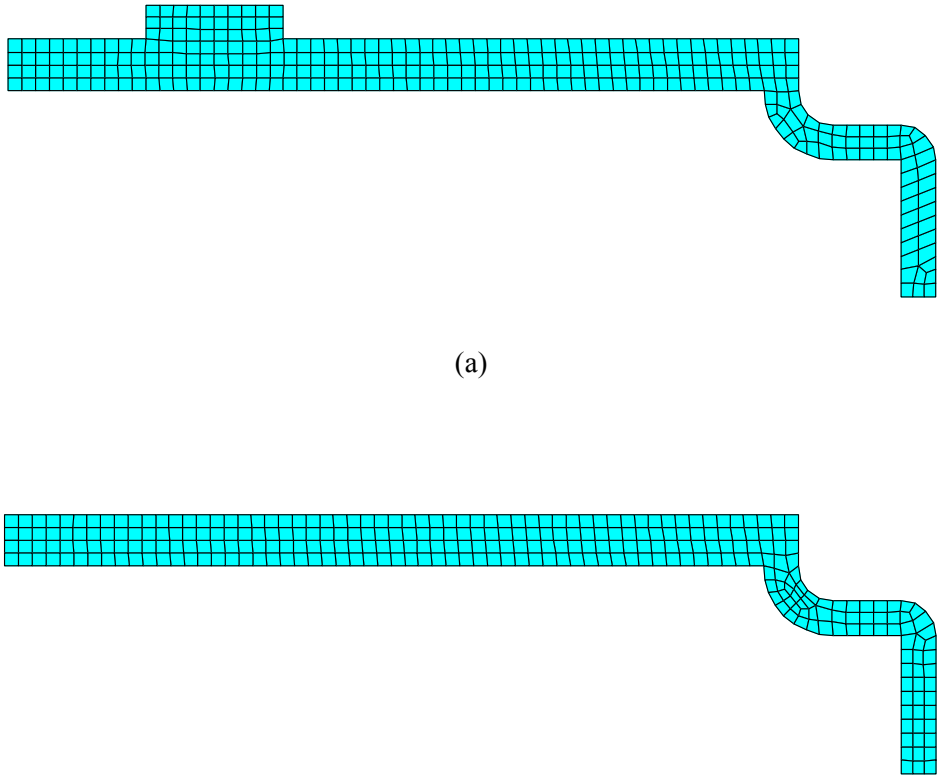

(a)

(b)

Figure 3.5: Section A-A cross-sectional view for (a) case 1 and (b) case 2

CHAPTER 4

RESULT AND DISCUSSION

4.1 ENERGY CONVERSION ANALYSIS

To investigate the temperature distribution, the brake hydraulic pressure is assumed constant and the pressure is equally distributed over the pad. Also, the truck deceleration is considered in constant rate along the braking period. In actuality, the hydraulic pressure may vary and the pressure distribution is not equal along the pad. The deceleration also might not in same rate due to non-constant pressure applied on the pad against drum inner surface. Figure 4.1 shows the time history of angular velocity, ω along braking period. The angular velocity is assumed to linearly decay from 56.63 rad/s and finally become zero at 5.66 second.

The energy conversion analysis is done based on dynamic movement of the truck during braking. Theoretically, moving truck stored kinematics energy. In order to stop the truck, the kinematics energy requires to be reduced in the moving body. Since energy cannot be eliminated, it is converted to other kind of energy which is heat energy. The brake system is the heating machine that converts the energy using sliding friction concept by rubbing the pad against drum inner surface. For this study, 100% of kinematics energy is converted to frictional heat and 95% of it is absorbed by the drum while the rest of 5% is absorbed by the brake pad. Figure 4.2 represents the accumulative heat energy absorbed by the drum. The heat energy absorbed increase in quadratic rate and achieved maximum of 1906.03 kJ. The values are obtained through the energy conversion calculation as demonstrated in Appendix C. Detail of data from iteration calculation over braking time is attached on Appendix E.

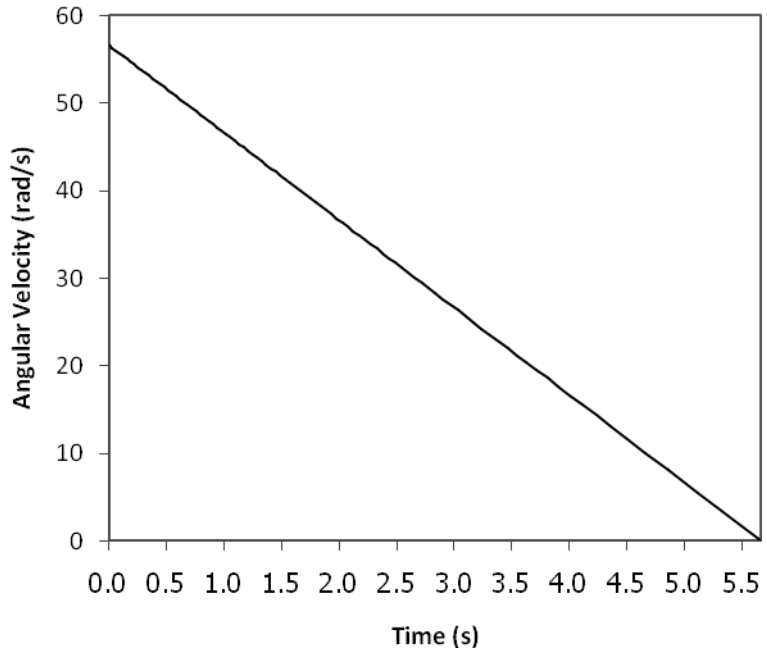

Figure 4.1: Time history drum angular velocity

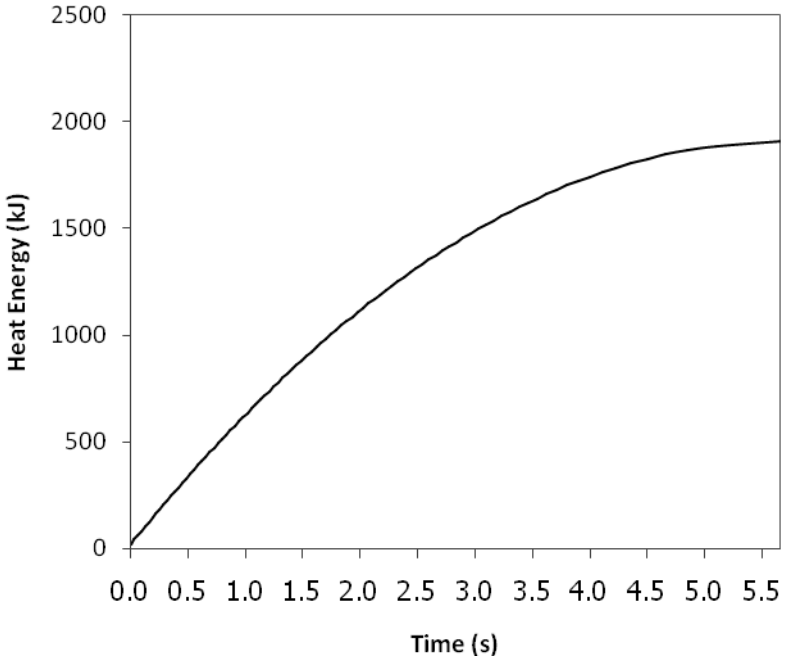

Figure 4.2: Accumulative heat energy absorbed by the drum

4.2 TEMPERATURE DEVELOPEMENT

The frictional heat created will result in temperature rise on the rubbing surface. At one point, it is subjected to heating and cooling alternately since there is a gap between first and second brake pad. 4 nodes and 2 nodes are selected at one drum cross-section for case 1 and case 2 respectively to investigate the temperature development along braking period as illustrated in Figure 4.3.

The value of heat energy absorbed is converted in heat flux form. Figure 4.4 shows the time history heat flux applied on drum rubbing surface. Highest heat flux with value of 4.53 MW/m^2 is generated at the beginning of the braking where the sliding is fastest. Then heat flux is linearly decreases because the truck is stopping at constant deceleration rate and finally reaches zero at the end of braking. These heat flux values are applied on the rubbing surface of simulation model at various period of time. The operation ambient temperature of 30^oC and the coefficient of convection considered is 51 $W/m^2.K$ based on reference experimental data.

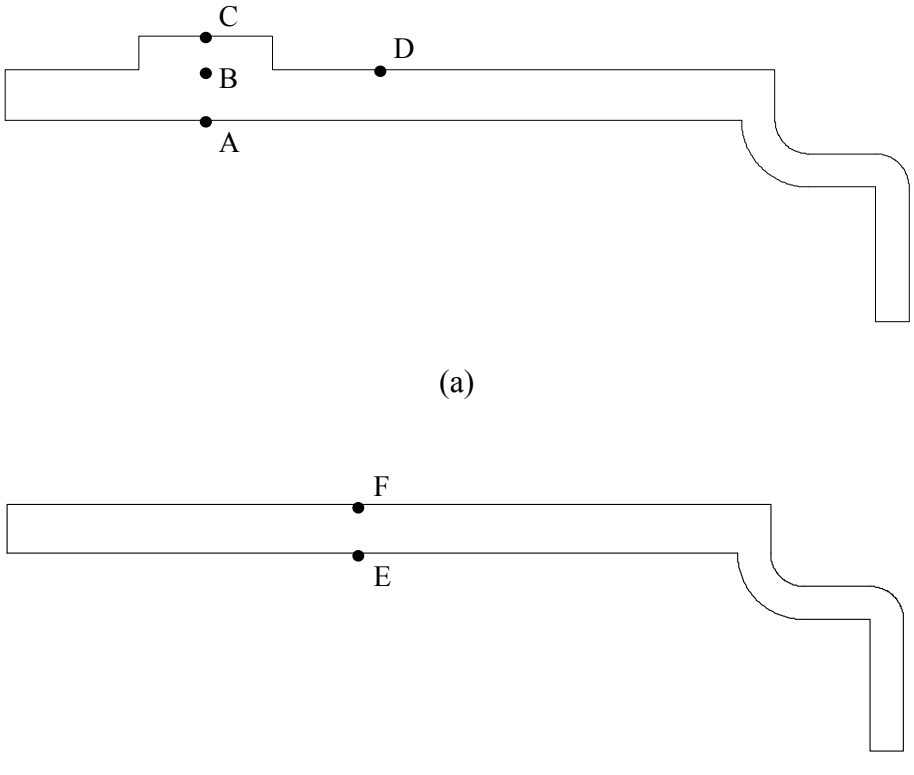

Figure 4.3: Selected point on drum cross-sectional of (a) case 1 and (b) case 2

The result of temperature development is represented Figure 4.5. It shows that temperature at node A where is located on the rubbing surface rise dramatically. The temperature increase is in fluctuating manner since the heating and cooling occur alternately. Whenever the pad is rubbing at one surface node, heat flux is occurred in direction from pad to drum inner surface and then it rises the temperature. While the pad is not makes contact, the node is cooled to the ambient air, resulting temperature drop.

Highest temperature is achieved at 2.6 second with value of 255^{o}C at node A. After that, the temperature drop back with final temperature of 185^{o}C at the end of braking. This occurred because the heat flux generated is decreasing and hence, less heat is absorbed. For node B, C and D, their highest temperature is 78^{o}C, 46^{o}C and 115^{o}C respectively which all of them are reached at the end of braking at 5.66 second.

For node E, the temperature development is exactly same as node A. Also for node F, the temperature history is just equal with the one at node D. This happen since they are located at the same thickness of drum although both Case 1 and Case 2 drum cross-section profile are different. However, temperature at node B is slightly lower than at node D even there are at the same thickness with same cross-section profile. Node B seems to have more capability to transfer the heat because all the heat is transferred via conduction. While at node D, more heat is dissipated to ambient air via convection which this method of transferring is less effective than conduction. As the result, temperature at node B becomes lower than node D due to fast and effective heat transfer. Node C has the lowest temperature because it is located at the furthest thickness as it takes longest time for heat to be transferred there.

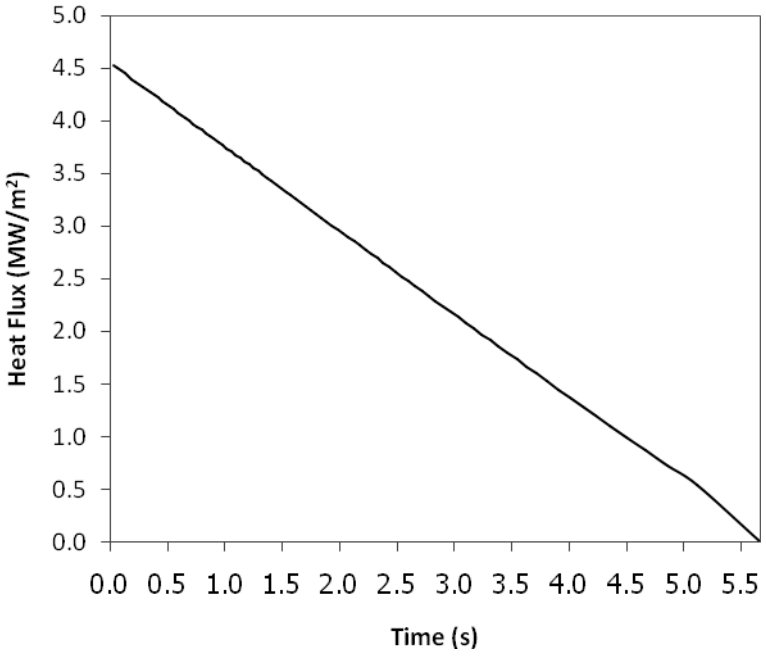

Figure 4.4: Time history heat flux generated along braking period

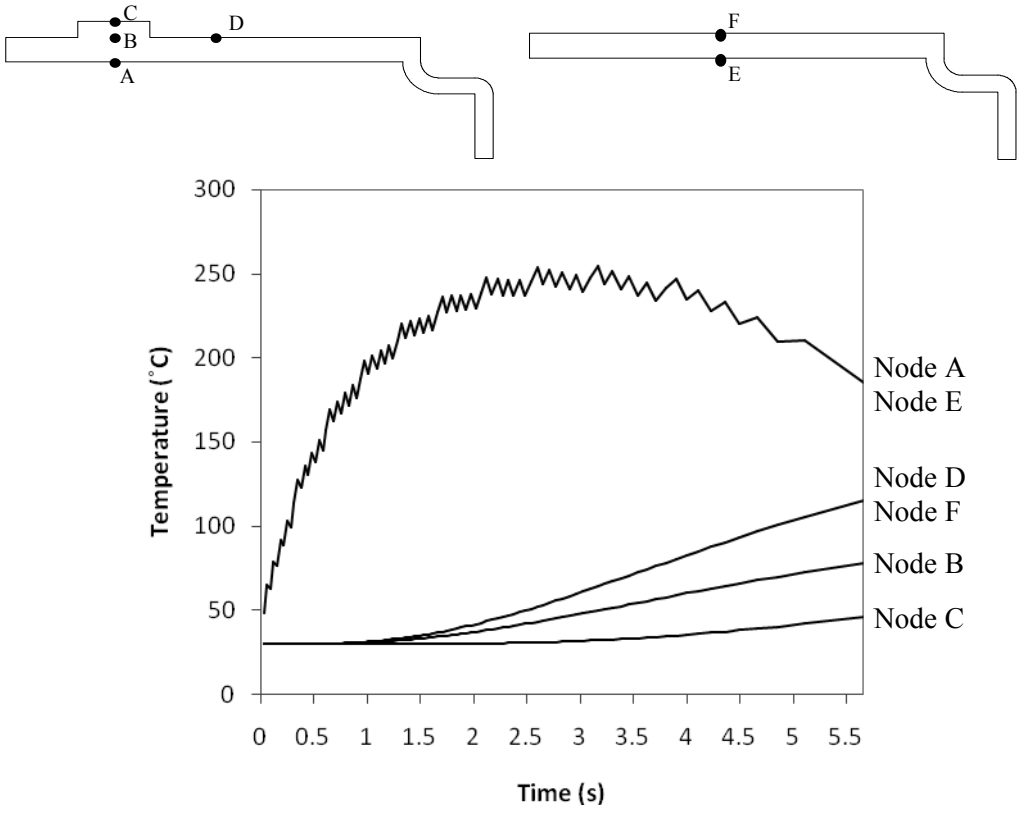

Figure 4.5: Time history temperature along braking period at selected nodes

4.3 TEMPERATURE DISTRIBUTION

The heat generated at the rubbing surface is transferred throughout drum body. For this study, the drum material is assumed homogenous. Thus, the temperature is expected to be well distributed within the material. Several paths from one node to node are defined to investigate the temperature distribution at one drum cross-section. Paths are defined as below and each node is shown in Figure 4.6.

- Path A (node 1 to 5) and Path B (node 7 to 11) will represent the path along the inner drum surface where heating take place.
- Path C (node 2 to 4 to 6) and Path D (node 8 to 12) will represent the path along the outer drum surface where convection cooling take place.
- Path E (node 3 to 4) represents the path from inner to outer surface at where the circumferential reinforcement is located.
- Path F (node 9 to 10) represents the path from inner to outer surface where there is no circumferential reinforcement.

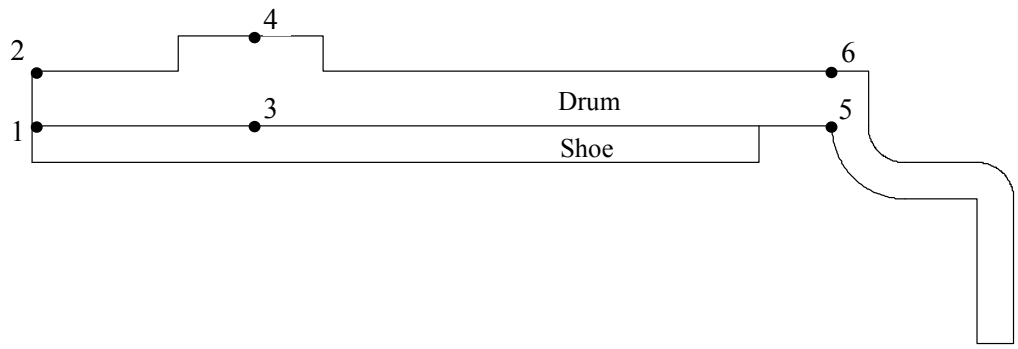

(a)

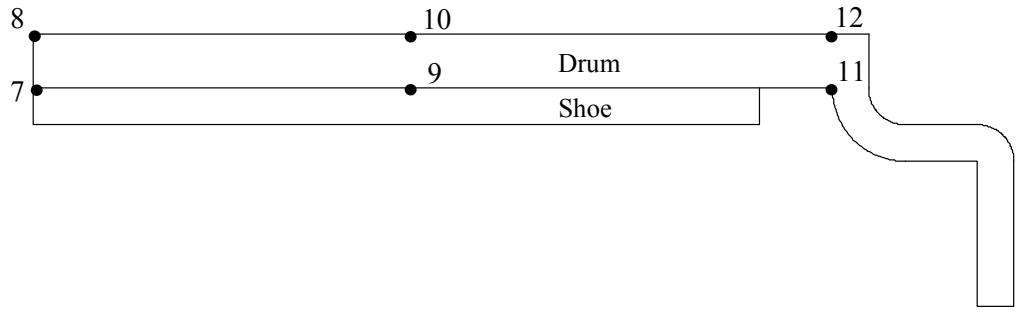

(b)

Figure 4.6: Nodes that defining the path for (a) case 1 and (b) case 2

4.3.1 Temperature along X-Axis Path

Horizontal path consist of Path A, Path B, Path C and Path D. The temperature at specific time is recorded along these paths in order to investigate the temperature distribution in the horizontal direction on inner and outer surface of the drum. Figure 4.7 shows the temperature distribution along Path A. The graph also shows the temperature distribution along Path B since the result recorded is just same as for Path A because both paths are located at where the frictional heat flux is applied due to pad rubbing against drum inner surface. This phenomenon shows that temperature distribution at rubbing surface is not affected by drum outer geometry but it does dependant on the value of heat flux applied and material properties. Since the material is assumed homogenous, the temperature remains constant along the path. However, at distance of 0.18 meter, the temperature starts to drop dramatically. It is happened because after the end of the path which at 0.22 meter distance, the temperature is still very low, resulting the heat start to be transferred earlier to the cooler adjacent molecules.

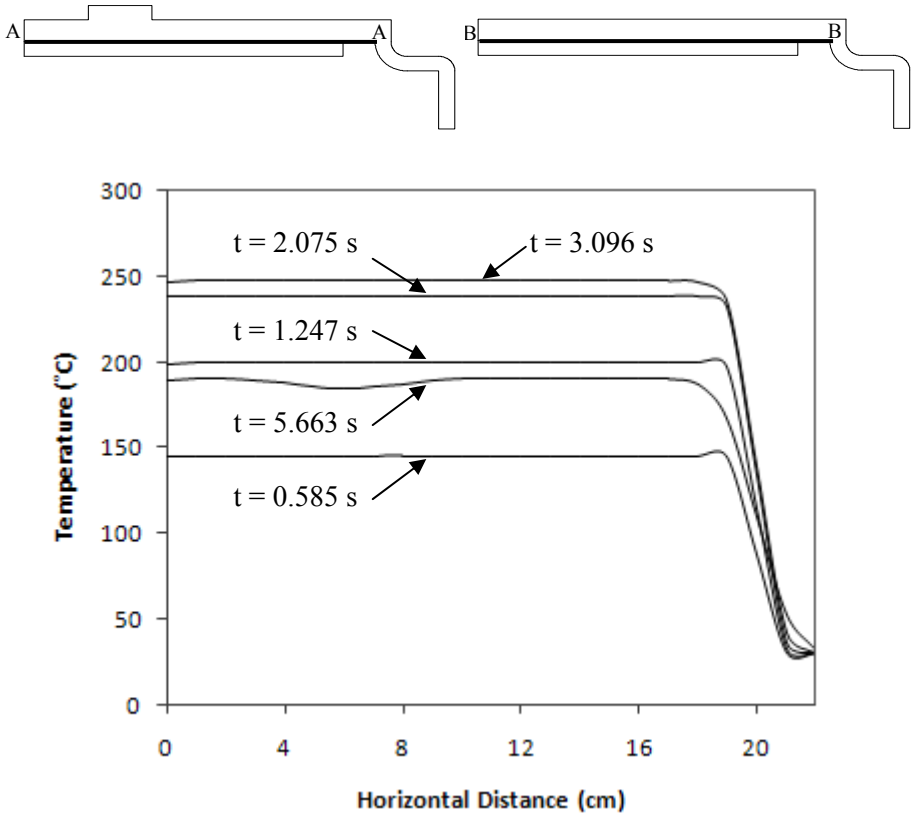

Figure 4.7: Temperature distribution along Path A and Path B

For Path C, the temperature distribution is as shown in Figure 4.8. At the same thickness, the temperature is constant along the line. But, at distance of 0.04 and 0.08 meter, the thickness is increase due to location of circumferential reinforcement. At greater thickness, the temperature rise of node is slower than the one at the lower thickness because more time is taken for heat to be transferred to the outer surface. As the result, the temperature starts to drop at distance of 0.028 meter and then rise back and settle to previous temperature at 0.097 meter. The cause of late temperature drop and rise is due to some of the heat is already transferred from hot to cool molecules slightly before the changes of geometry. Different phenomenon happened for Path D where the temperature is constant along the path since there is no change at outer geometry. The temperature distribution for Path D is shown in Figure 4.9.

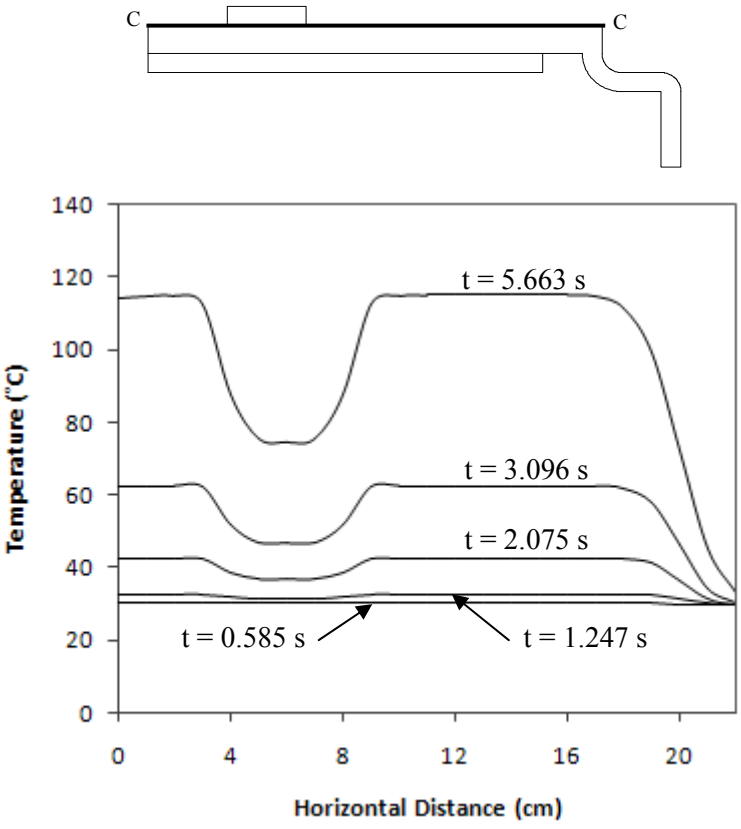

Figure 4.8: Temperature distribution along Path C

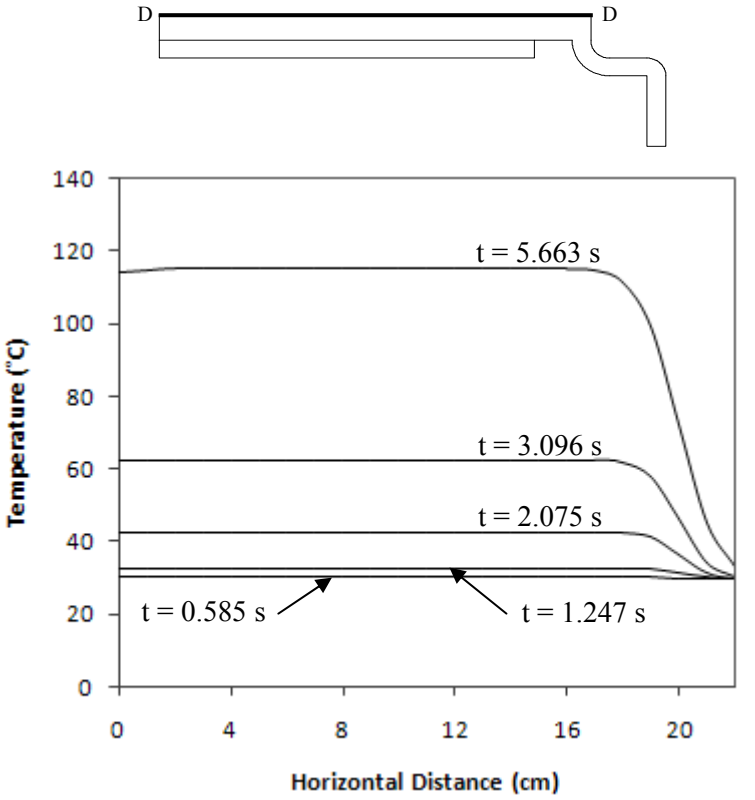

Figure 4.9: Temperature distribution along Path D

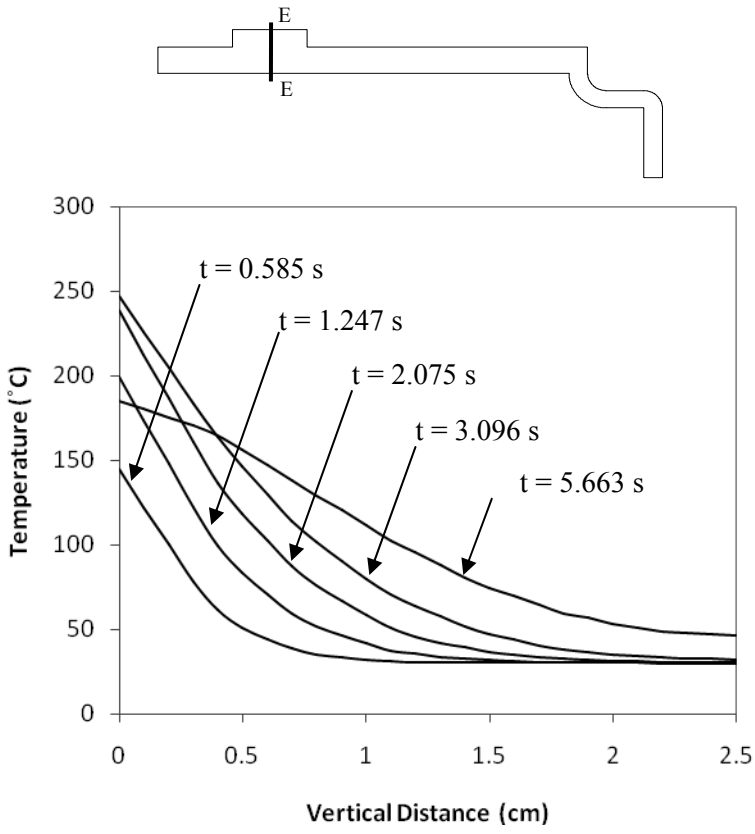

Figure 4.10: Temperature distribution along Path E

4.3.2 Temperature along Y-Axis Path

Vertical path consist of Path E and Path F. The temperature along these paths is investigated to observe its distribution from inner to outer surface of the drum. The temperature distribution also is recorded at same specific time as in vertical path. From Figure 4.10, highest temperature for Path E is experienced at distance of 0.0 meter at any time because here is where the frictional heat flux application takes place. Then, the temperature gradually drops as the thickness increase. The temperature is far lower at the end of the thickness because the rate of heating at rubbing surface is a lot faster than the heat is transferred.

Same situation happen for Path F as shown in Figure 4.11. However, at same vertical distance, Path F experienced higher temperature than it is at Path E. This happen because Path E have extra thickness with cooler temperature that promote effective heat transfer via conduction. As the result, the temperature difference between thicknesses for Path E is larger than Path F, with same maximum temperature at 0.0 meter distance.

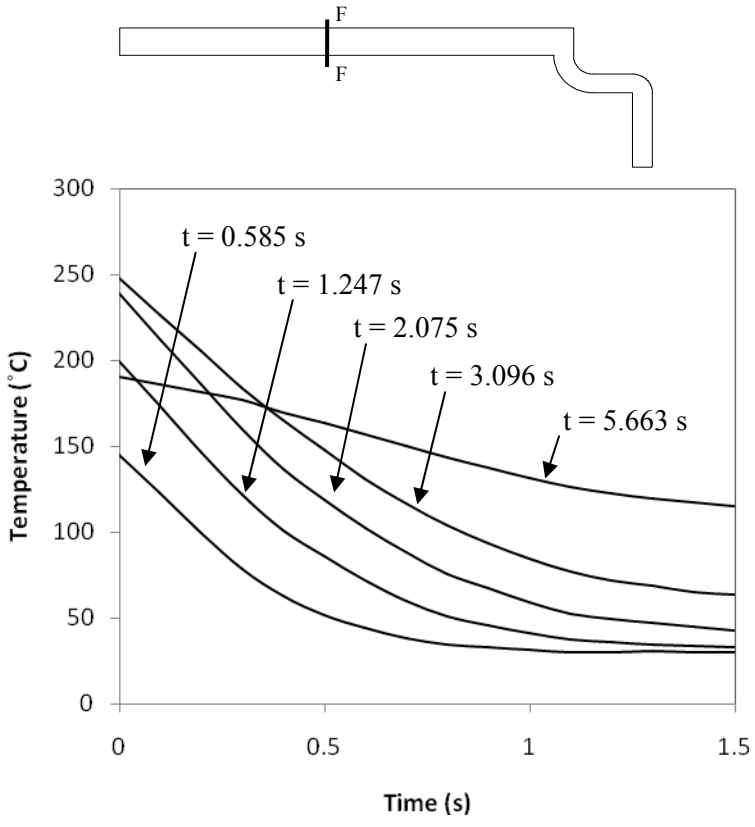

Figure 4.11: Temperature distribution along Path F

4.4 TEMPERATURE CONTOUR

Temperature contour for brake drum are plotted various braking time to observe in the temperature distribution in clearer view. The temperature contour on drum surface and drum cross-sectional area for case 1 and 2 is shown in Appendix H.

4.5 THERMAL STRESS DEVELOPMENT

The frictional heat created will result in temperature rise on the rubbing surface. At one point, it is subjected to heating and cooling alternately since there is a gap between first and second brake pad. 4 nodes and 2 nodes are selected at one drum cross-section for case 1 and case 2 respectively to investigate the thermal stress development along braking period as illustrated in Figure 4.3.

The result of thermal stress development is represented Figure 4.12. It shows that temperature at node A where is located on the rubbing surface rise dramatically. The temperature increase is in fluctuating manner since the temperature occurs alternately based on rubbing surface of the brake pad at different time. Whenever the pad is rubbing at one surface node, then it raises the temperature that make the thermal stress rise as well. While the pad is not makes contact, the node is cooled to the ambient air, resulting temperature drop will make the thermal stress drop.

Highest thermal stress occurs at node A. It is achieved at 1.32 second with value of 93 MPa. After that, the thermal stress drop back with final thermal stress of 4.9 MPa at the end of braking. For node B, C and D, their highest thermal stress is 21 Mpa at 3.1 second, 44 Mpa at 2.72 second and 38 Mpa at 1.71 second respectively.

For node F, the thermal stress development is exactly same as node D. This happen since they are located at the same thickness of drum although both Case 1 and Case 2 drum cross-section profile are different. However, thermal stress at node E is lower than at node A, this is because for case 1 where the node A located. In the case 1, they have circumferential reinforcement which more thickness than case 2 where node E located. As the result, the thermal stress at node E becomes lower than node A due to fast and effective heat transfer. The thermal stress development for node E and F is shown in the Figure 4.13.

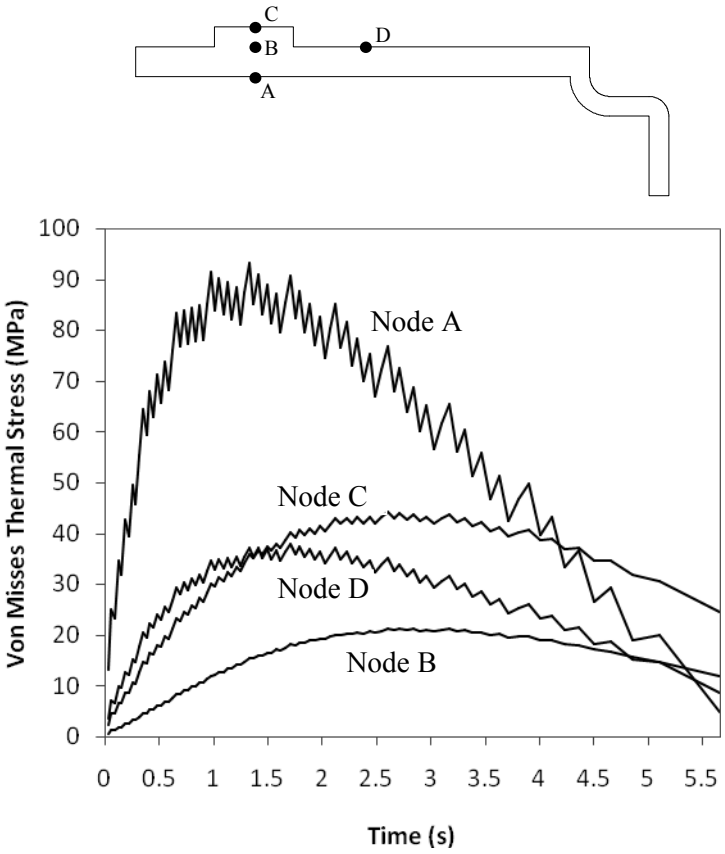

Figure 4.12: Time history thermal stress along braking period at node A, B, C and D

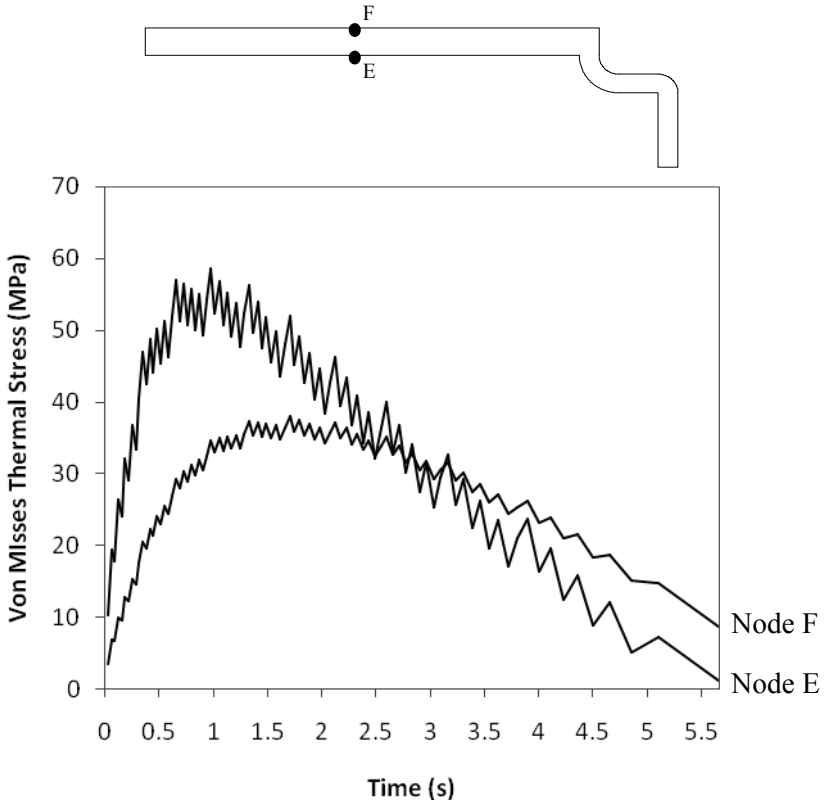

Figure 4.13: Time history thermal stress along braking period at node E and F

4.6 THERMAL STRESS DISTRIBUTION

The temperature generated at the rubbing surface is transferred throughout drum body. Thus, the temperature is distributed within the material. Several paths from node to node are defined to investigate the thermal stress distribution at one drum cross-section. Paths are defined as shown in Figure 4.6.

4.6.1 Thermal Stress along X-Axis Path

Horizontal path consist of Path A, Path B, Path C and Path D. The temperature at specific time is recorded along these paths in order to investigate the thermal stress distribution in the horizontal direction on inner and outer surface of the drum. Figure 4.14 & Figure 4.15 shows the thermal stress distribution along Path A and Path B respectively. The graph shown that, the thermal stresses of Path A are rising at the distance of 4 to 8 centimeter in horizontal distance where the circumferential reinforcement is located. It shows that, the temperature dissipated faster at this area. Therefore the temperature change is high due to the temperatures dissipated which make the thermal stress rise at this area. For the Figure 4.15, the thermal stress distribute equally along the rubbing surface due to the geometry of the drum in case 2. However, at distance of 18 centimeter, the temperature starts to drop dramatically. It is happened because after the end of the path which at 20 centimeter distance, the temperature is still very low, resulting the heat start to be transferred earlier to the cooler adjacent molecules.

For Path C, the thermal distribution is as shown in Figure 4.16. At the same thickness, the temperature is constant along the line. But, at distance of 4 and 8 cm, the thickness is increase due to location of circumferential reinforcement. At greater thickness, the temperature rise of node is slower than the one at the lower thickness because more time is taken for heat to be transferred to the outer surface. As the result, the thermal stress starts to drop at distance of 4 cm and then rise back and settle to previous temperature at 8 cm. The cause of late temperature drop and rise is due to some of the heat is already transferred from hot to cool molecules slightly before the changes of geometry. Different phenomenon happened for Path 4 where the thermal stress is constant along the path since there is no change at outer geometry. The temperature distribution for Path D is shown in Figure 4.17.

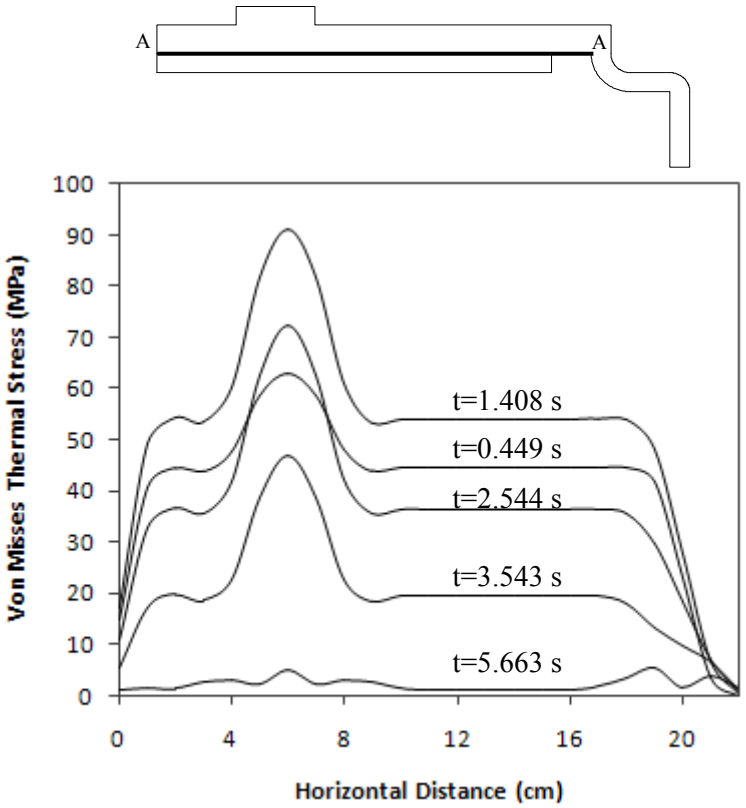

Figure 4.14: Thermal stress distribution along Path A

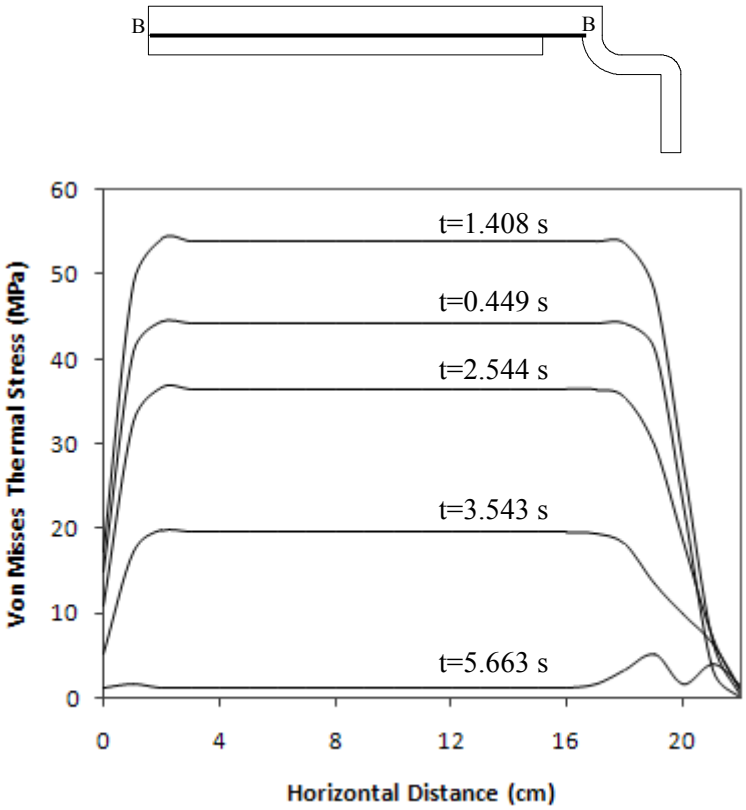

Figure 4.15: Thermal stress distribution along Path B

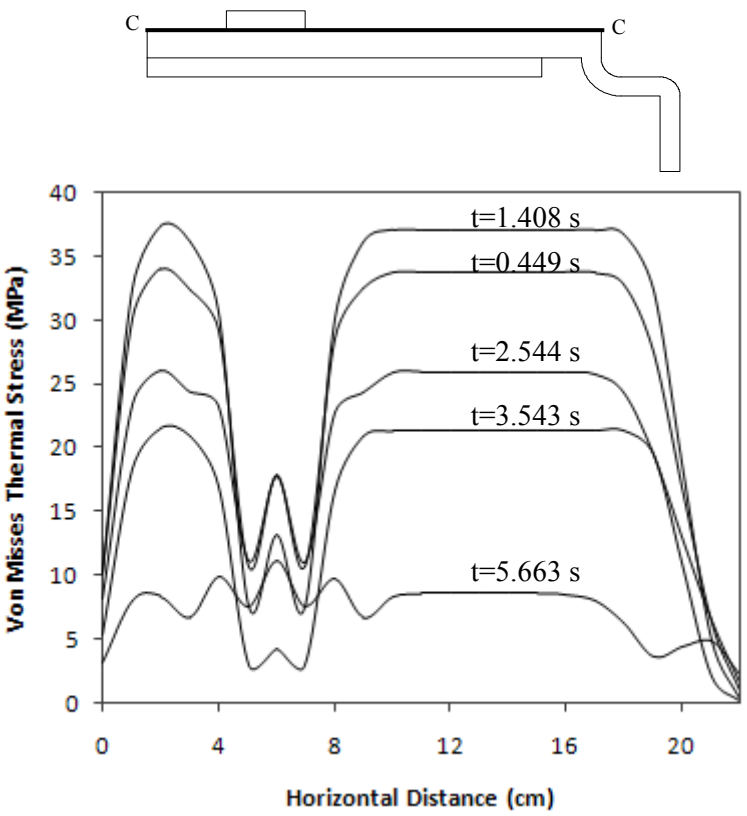

Figure 4.16: Thermal stress distribution along Path C

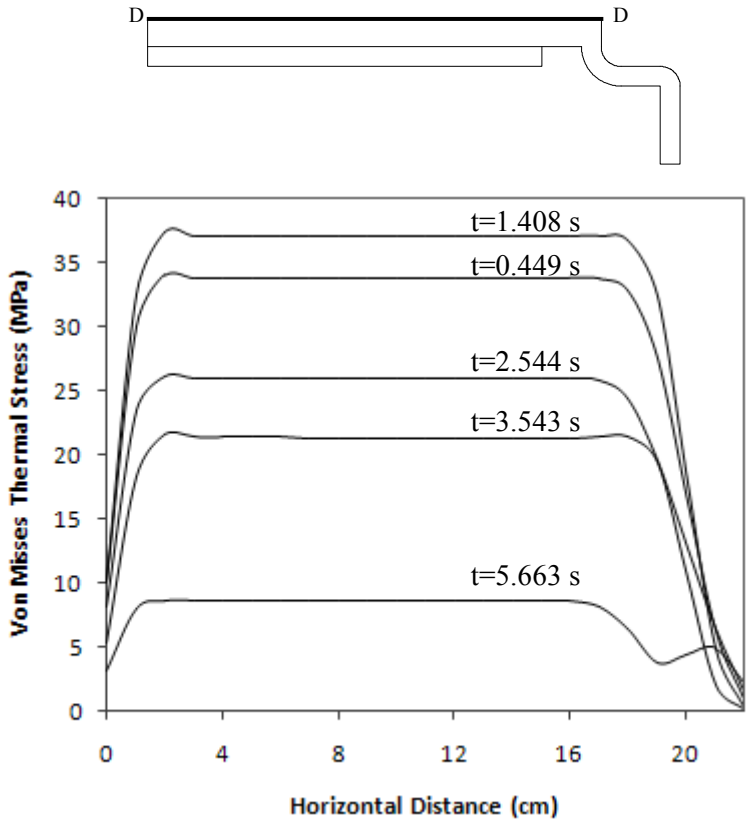

Figure 4.17: Thermal stress distribution along Path D

4.6.1 Thermal Stress along Y-Axis Path

Vertical path consist of Path E and Path F. The temperature along these paths is investigated to observe its distribution from inner to outer surface of the drum. The thermal stress distribution also is recorded at same specific time as in vertical path. From Figure 4.17, highest thermal stress for Path E is experienced at distance of 0 centimeter at any time because here is where the frictional heat flux application takes place. Then, the thermal stress gradually drops as the thickness increase. And then start to rise up and drop down at the thickness of 0.5 to 1.9 centimeters because the rate of heating at rubbing surface is a lot faster than the heat is transferred. And it rise up again until the end of braking period.

Same situation happen for Path F as shown in Figure 4.18. The trend of thermal stress is the same. However, Path F experienced lower thermal stress than Path E. This happen because Path E have extra thickness with cooler temperature that promote effective heat transfer via conduction that make more temperature changed which lead to the higher thermal stress.

4.7 THERMAL STRESS CONTOUR

Thermal stress contour for brake drum are plotted various braking time to observe in the stress distribution in clearer view. The thermal stress contour on drum surface and drum cross-sectional area for case 1 and 2 is shown in Appendix I.

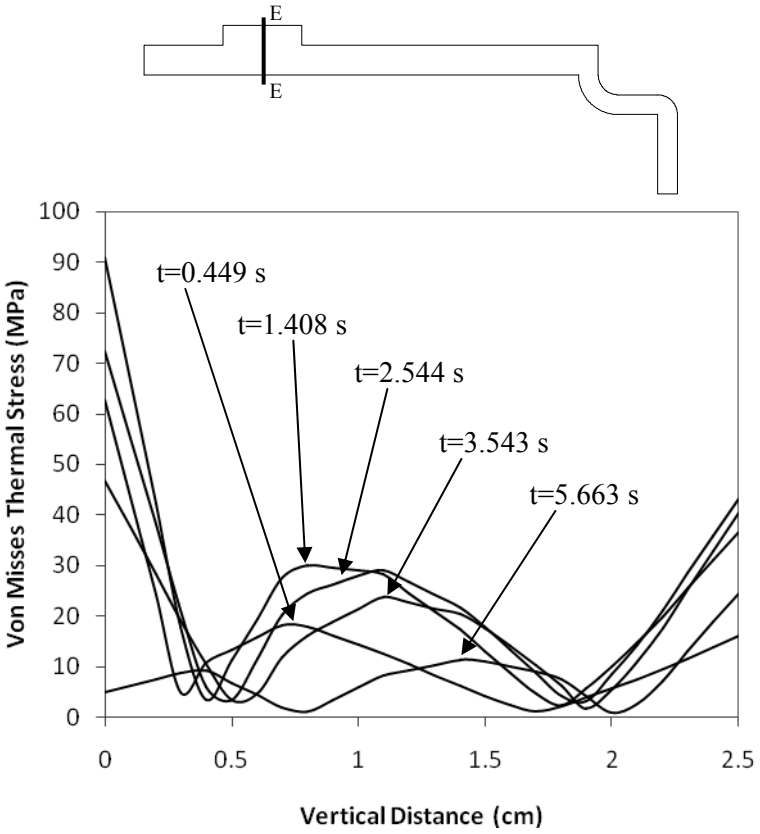

Figure 4.18: Thermal stress distribution along Path E

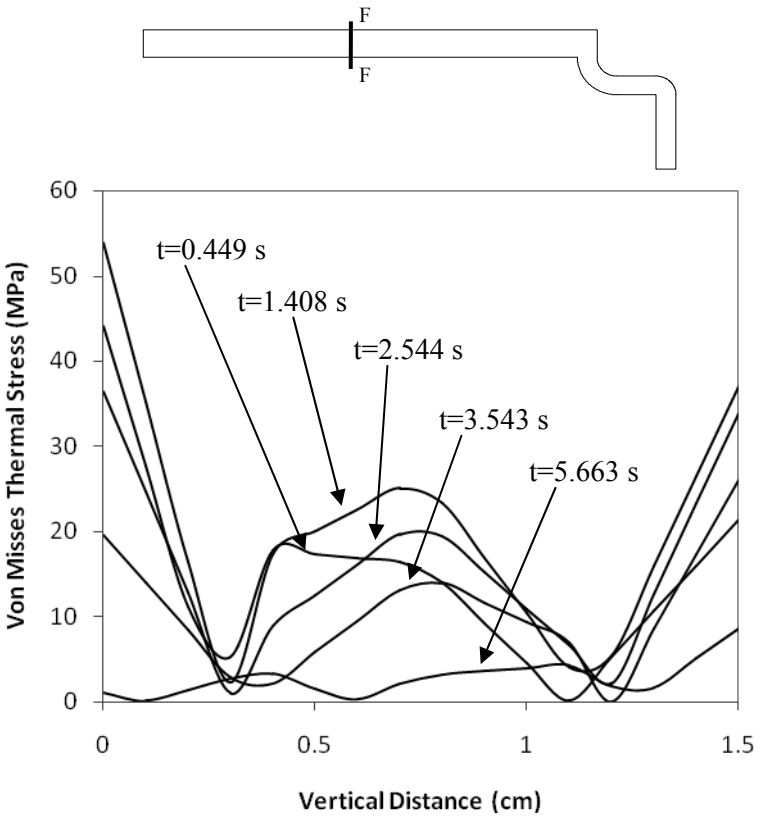

Figure 4.19: Thermal stress distribution along Path F

4.8 THERMAL EXPANSION DEVELOPMENT

The thermal expansion is strongly dependant to the temperature. It will increase as the temperature increase. The most effective of the thermal expansion is where the highest temperature is. Therefore, at the inner of the brake drum is most effect of the thermal expansion where the located of the rubbing surface. As the result of the thermal expansion shown in the Figure 4.20, it shows that the thermal expansion rise dramatically and it achieved the maximum displacement of 2.87 millimeters at 2.72 second and 0.45 millimeters at 3.9 second of braking period in X and Y direction respectively. The thermal expansion in Y direction for Case 1 is just slightly higher than Case 2 while the displacement in X direction is exactly the same. This is because the temperature generated on the rubbing surface in the case 1 takes longer time to transfer the temperature to the outer surface due to the geometry of the drum in case 1 including with the circumferential reinforcement that will make longer in thickness as compared to the case 2. Therefore, the temperature difference between outer and inner surface in Case 2 is lesser than case 1 which lead to lower thermal expansion.

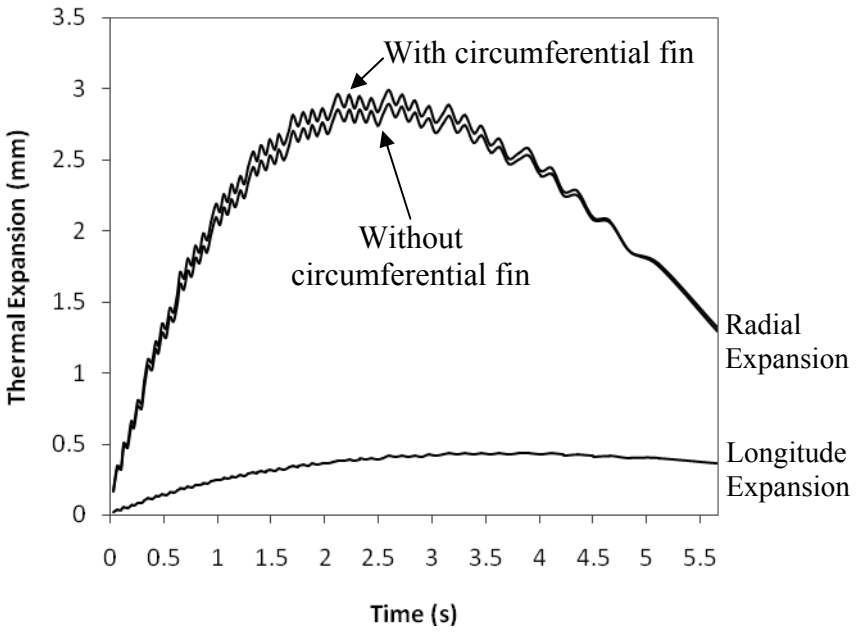

Figure 4.20: Time history thermal expansion at the free edge of brake drum in the course of braking

4.9 THERMAL EXPANSION CONTOUR

Thermal expansion contour for brake drum are plotted various braking time to observe the thermal stress distribution in clearer view. The thermal expansion contour on drum surface and drum cross-sectional area for case 1 and 2 is shown in Appendix J.

CHAPTER 5

CONCLUSION AND RECOMMENDATION

5.1 CONCLUSION

Based on the theoretical and simulation investigations in this study, the following observations and conclusions are made:

- The estimated time duration to stop the truck under severe braking condition is 5.66 s. During this time period, maximum temperature on drum rubbing surface is achieved up to 255^{o}C in the middle of braking period at 2.6 s. However, at outer surface of drum, maximum temperature reached at the end of braking with value of just 115^{o}C.
- Nodes with all-direction to conduct heat to surrounding adjacent cooler node transfer the heat at faster rate than node with more direction to dissipate it to air instead of conducting it.
- The temperature at inner surface is unequally distributed along the heating line where brake lining and drum make contact. At outer surface, the temperature also equally distributed along the line. But, the temperature level will change as there is geometry variant with different thickness.
- The maximum thermal stress achieved 93 MPa by 1.32 s after braking started at the rubbing surface and at the outer surface thermal stress achieved 38 MPa at 1.71 s.
- Thermal stress increase when the thickness increase due to the heat transfer rate is faster.
- At the rubbing surface, thermal expansion has more effect to the displacement due to higher temperature generated.

5.2 RECOMMENDATION

The following recommendations are presented to further improve the understanding of thermal stress and expansion rise and distribution in brake drum.

- No data validation and comparison is made in this study due to no experimental data. In the future, the experiment for observing the temperature development and its distribution should be conducted to validate the simulation results approximation.
- Braking phenomenon is not well understood and many assumptions are made in this study. The analysis with thermal properties that varies with temperature, inconsistent brake pressure and coefficient of friction and thermo elastic instability consideration may be useful to improve the approximation to real braking condition.
- In this study, only thermal effect and drum design is proposed and investigated. In next study, more case should be made and more uncertainty should be considered. This really helpful in improving the brake design and performance.
- Three-dimensional analysis method quite consuming time and higher computer requirement is required. If possible, the method is reduced to two-dimensional analysis without affecting the results obtained in three-dimensional method.

REFERENCES

1) G. Budinski, K. Budinski, Engineering Material – Properties and Selection, 7th Edition, 2002, Prentice Hall.
2) Frank P. Incropera, David P. Dewit, Introduction to Heat Transfer, 4th Edition, 2002, John Wiley & Sons.
3) V.Linck, A. Saulot, L.Baillet, Consequence of contact local kinematics of sliding bodies on the surface temperatures generated, Elsevier, Tribology International 39 (2006) 1664-1673.
4) J.H.Choi, I.Lee, Finite element analysis of transient thermoelastic behaviors in disk brakes, Elsevier, Wear 257 (2004) 47-58.
5) K.Lee, Frictionally excited thermoelastic instability in automotive drum brakes, ASME, Journal of Tribology 122 (2000) 849-855.
6) R.C. Hibbeler, Engineering Mechanics – Dynamics, 2nd Edition in SI Units, 2001, Prentice Hall.
7) Yunus A. Cengel, Heat Transfer – A Pratical Approach, 2nd Edition in SI Units, 2004, Mc Graw Hill.
8) A.Hattiangadi, T.Siegmund, A numerical study on interface crack growth under heat flux loading, Elsevier, International Journal of Solids and Structures 42 (2005) 6335-6355.
9) H.Zaidi, A.Senouci, Thermal tribological behavior of composite carbon metal/steel brake, Elsevier, Applied Surface Science 144-145 (1999) 265-271.
10) B.K. Servis, The Onset of Squeal Vibrations in Drum Brake Systems Resulting from a Coupled Mode Instability, Ph.D. Thesis, Purdue University, West Lafayette, IN, 2000.
11) M.Naji, M.Al-Nimr, Dynamic thermal behavior of a brake system, Pergamon, Int. Comm. Heat Mass Transfer Vol 28 (2001) 835-845.
12) Saeed Moaveni, Finite Element Analysis – Theory and Application with ANSYS, 2nd Edition, 2003, Pearson Education.
13) C.H.Gao, X.Z.Lin, Transient temperature field analysis of a brake in a non-axisymmetric three-dimensional model, Elsevier, Journal of Materials Processing Technology 129 (2002) 513-517.

14) A.Ilinca, F.Ilinca, B.Falah, Numerical and analytical investigation of temperature distribution in a brake drum with simulated defects, Inderscience, International Journal of Vehicle Design 26 (2001) 146-160.
15) J.Erjavec, Don Knowles, Medium/Heavy Duty Truck Brakes, 2003, Delmar Publisher.
16) DOE Fundamental Handbook – Thermodynamics, Heat Transfer and Fluid Flow, Vol 2 of 3, US Department of Energy, Washington DC.
17) Jaluria, Torrance, Computational Heat Transfer, 2nd Edition, 2003, Taylor and Francis Publisher
18) Manual of Truck Tyre Basics, Continental
19) Manual of Gunite Heavy-Duty Brake Drums – Maintenance and Installation, Gunite Corporation.

APPENDIX A

Drum Material failure

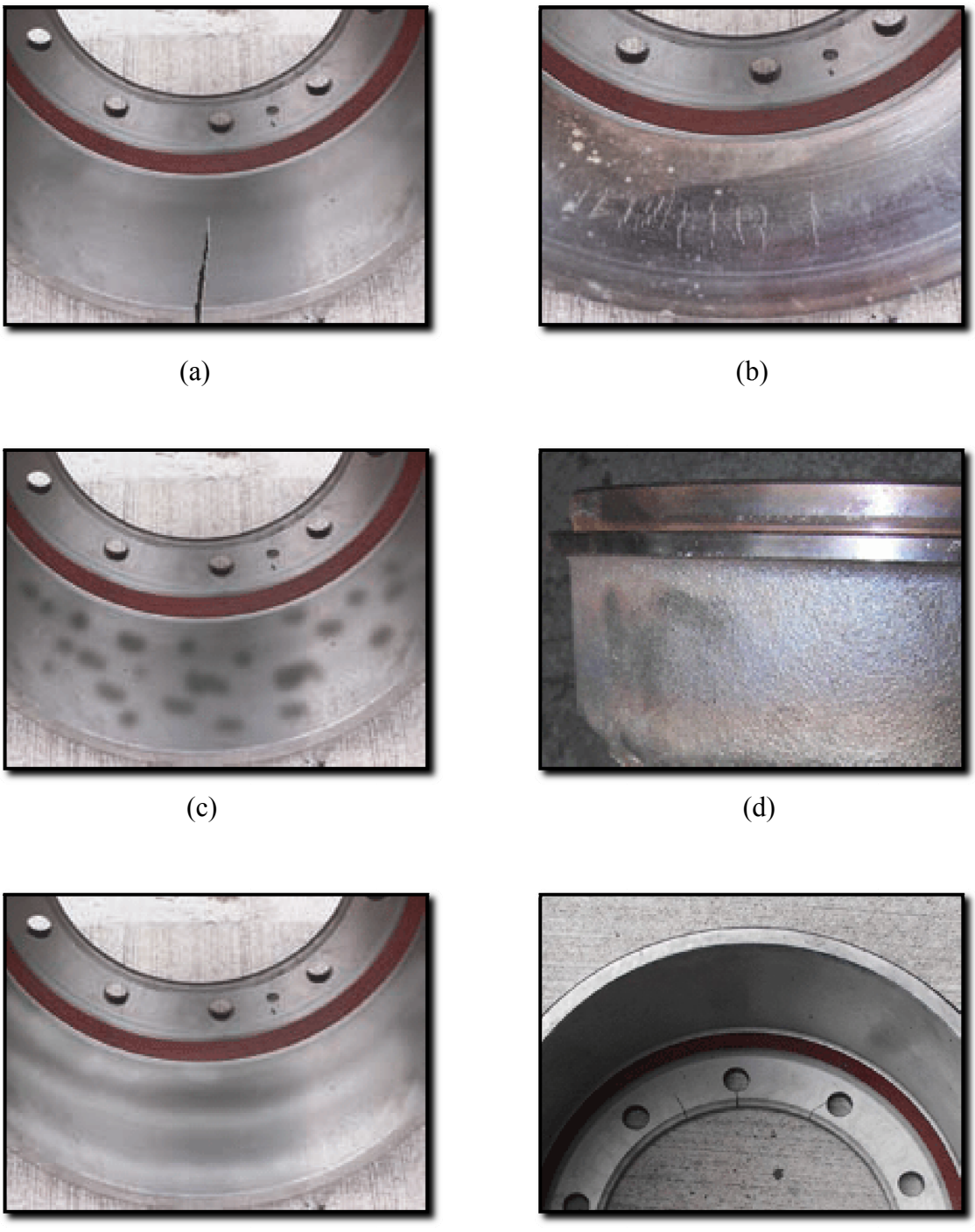

(a) (b)

(c) (d)

(e) (f)

Figure A: Illustration of (a) thru-crack, (b) heat-check, (c) martensile spotted, (d) blue drum, (e) excessive wear and (f) radial crack

APPENDIX B

Drum Dimension

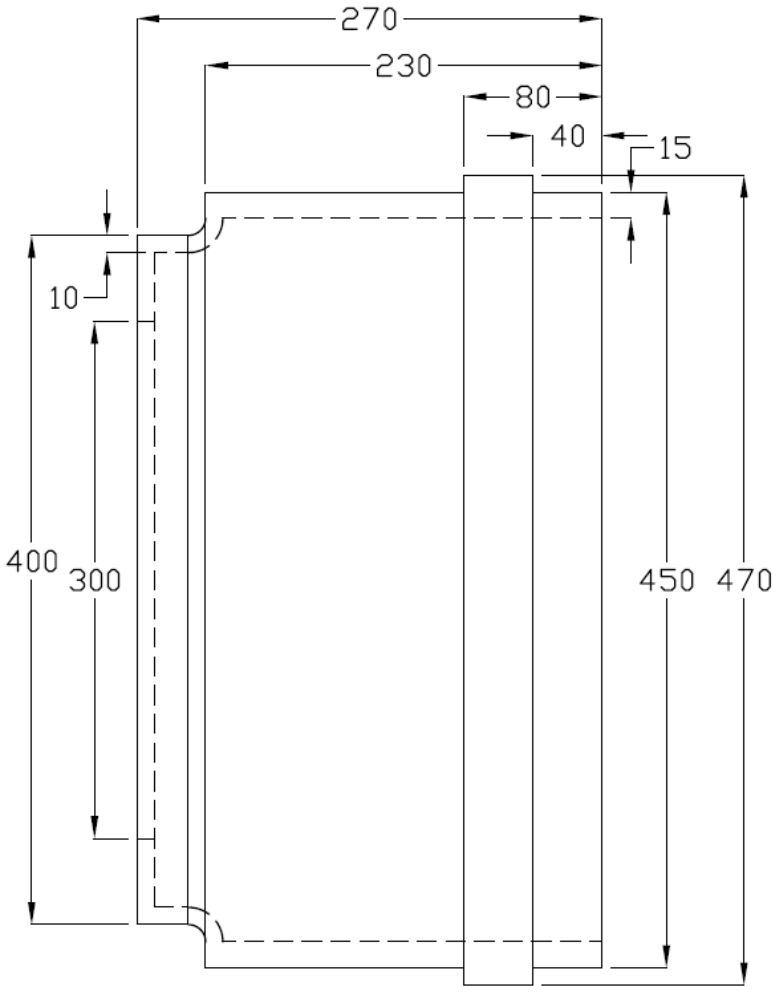

Side View

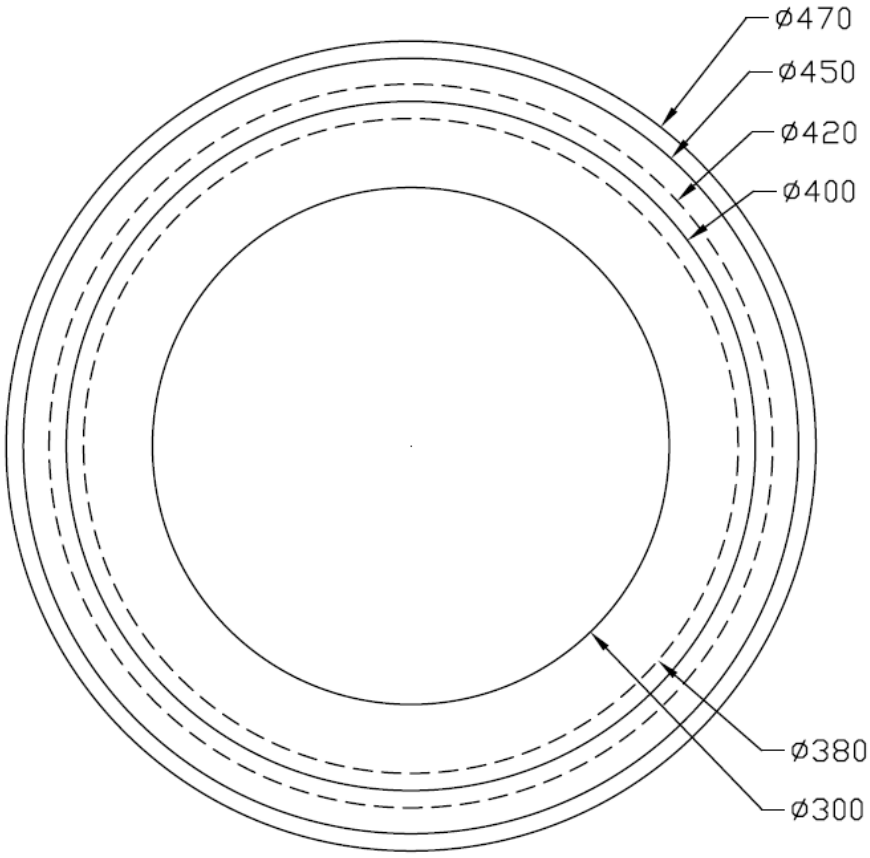

Front View

Note: All units in mm.

APPENDIX C

Sample calculation of truck and drum dynamic analysis

- **KINETICS AND DYNAMICS PROBLEM**

$v = 0$ km/h

$u = 100$ km/h = (100 km/h)(1000 m/km)(h/3600 s) = 27.778 m/s

$a = 0.5g = 0.5(9.81\ m/s^2) = 4.905\ m/s^2$

1) Time taken to fully stop the truck (*t*)

From Equation of Rigid Body in Rectilinear Motion

$$v = u + at$$

Substitute; $0 = 27.778 + (-4.905)\ t$

Therefore, $t = 5.663$ s

2) Distance traveling of the truck when fully stop (*s*)

From Equation of Rigid Body in Rectilinear Motion

$$v^2 = u^2 + 2as$$

Substitute; $0 = (27.778)^2 + 2(-4.905)\ s$

Therefore, $s = 78.656$ m

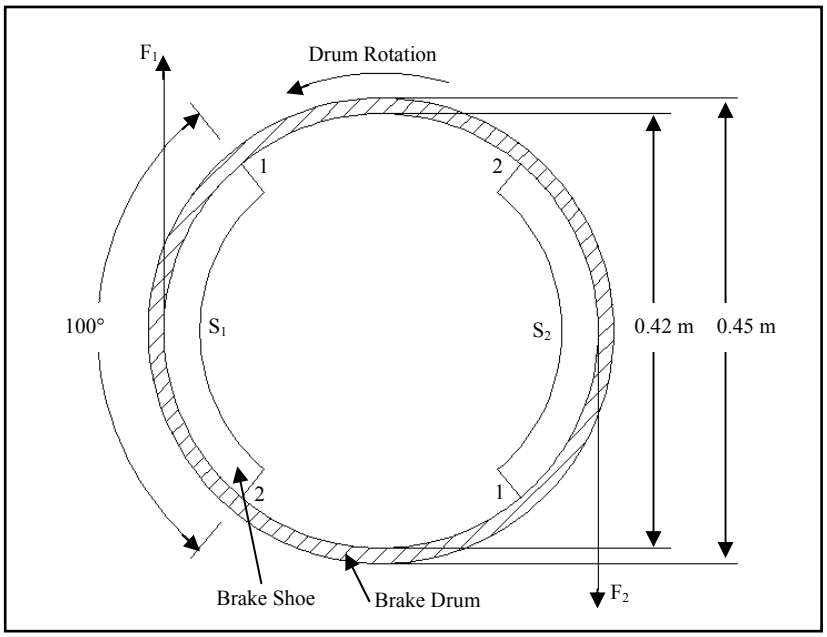

Figure 1: Free-Body Diagram of brake drum during braking condition

3) **Shoe contact area (*A*)**

From $A = s_{1-2} \times w$

$$A = \frac{d_i \theta \Pi}{180} \times W$$

$$A = \frac{0.42 \times 100 \times \Pi}{180} \times 0.2$$

$$A = 0.147 \ \text{m}^2$$

- **EQUATION OF RIGID BODY MOTION ABOUT A FIXED AXIS**

4) Initial angular velocity of drum (ω)

From Equation of Rigid Body Motion about a Fixed Axis:

$$v_t = \frac{1}{2} D\omega_0$$

Substitute; $27.778 = \frac{1}{2}(0.981)\,\omega_0$

Therefore, $\omega_0 = 56.632$ rad/s

5) Angular deceleration of drum (α)

From Equation of Rigid Body Motion about a Fixed Axis:

$$a_t = \frac{1}{2} D\alpha$$

Substitute; $4.905 = \frac{1}{2}(0.981)\,\alpha$

Therefore, $\alpha = 10.00$ rad/s^2

6) Angular velocity of the next shoe movement

From $\omega_1^2 = \omega_0^2 + 2\alpha\theta$

$$\omega_1 = \sqrt{\omega_0^2 + 2\alpha\theta}$$

$$\omega_1 = 56.3229 \text{ rad/s}$$

(*note: Calculation must be continues until value of ω becomes zero)

7) Time interval between shoe movement

From $\omega_1 = \omega_0 + \alpha t$

$$\Delta t = \frac{\omega_1 - \omega_0}{\alpha}$$

$$\Delta t = \frac{56.3229 - 56.6316}{-10}$$

$$\Delta t = 0.0309 \text{ s}$$

(*note: Calculation must be continues until value of ω becomes zero)

- **WORK AND ENERGY PROBLEM**

Theoretically, the kinetic energy defined as;

$$T_1 + \Sigma U_{1\text{-}2} = T_2$$

and $$T = \frac{1}{2}mv^2$$

Since, final velocity is 0 (when it fully stops)

Therefore, the final kinetic energy (T_2) is 0.

$$T = -\Delta U_{1-2}$$

$$\frac{1}{2}mv^2 = -Fs$$

8) Force Required to stop the truck

m = 40000 kg

v = 27.778 m/s

s = 78.656 m

Substitute into: $\frac{1}{2}mv^2 = -Fs$

$$\frac{1}{2}(40000)(27.778)^2 = \text{-F } (78.656)$$

Therefore; F = 196.2 kN

9) Frictional force acting on rubbing surface of one front brake drum

From $F_{fr} = 0.3F$

$F_{fr} = 0.3(196.2)$

Therefore; $F_{fr} = 58.86$ kN

10) Heat energy absorbed by drum

From $\Delta Q = 0.95 F_{fr} s_{1-2}$

Substitute; $\Delta Q = 0.95 \times 58.86 \times 10^3 \times \left(\frac{0.42 \times 100\Pi}{2 \times 180} \right)$

$\Delta Q = 20.4949$ kJ

(*note: Calculation must be continues until value of ω becomes zero)

11) Heat flux generated on one break shoe

From $q = \frac{1}{2}\left(\frac{\Delta Q}{A \Delta t} \right)$

$q = \frac{1}{2}\left(\frac{20.4949 \times 10^3}{0.0733 \times 0.0309} \right)$

$q = 4.5287$ MW/m^2

(*note: Calculation must be continues until value of ω becomes zero)

APPENDIX D
Detail Data for Energy Conversion analysis

No. of shoe movement	Time Interval (second)	Total time (second)	Agular velocity (rad/s)	Instantaneous heat energy (kJ)	Accumulative heat energy (kJ)	Heat flux per shoe (MW/m2)
0	0.0000	0.0000	56.6316	20.4949	20.4949	0.0000
1	0.0309	0.0309	56.3229	20.4949	40.9898	4.5287
2	0.0311	0.0619	56.0122	20.4949	61.4847	4.4990
3	0.0312	0.0932	55.6997	20.4949	81.9796	4.4741
4	0.0314	0.1246	55.3855	20.4949	102.4745	4.4490
5	0.0316	0.1562	55.0694	20.4949	122.9694	4.4237
6	0.0318	0.1880	54.7516	20.4949	143.4643	4.3983
7	0.0320	0.2200	54.4319	20.4949	163.9592	4.3728
8	0.0322	0.2521	54.1103	20.4949	184.4541	4.3471
9	0.0324	0.2845	53.7868	20.4949	204.9490	4.3213
10	0.0325	0.3170	53.4613	20.4949	225.4439	4.2953
11	0.0327	0.3498	53.1338	20.4949	245.9388	4.2692
12	0.0329	0.3827	52.8043	20.4949	266.4337	4.2428
13	0.0332	0.4159	52.4728	20.4949	286.9286	4.2164
14	0.0334	0.4493	52.1391	20.4949	307.4235	4.1897
15	0.0336	0.4828	51.8032	20.4949	327.9184	4.1629
16	0.0338	0.5166	51.4652	20.4949	348.4133	4.1359
17	0.0340	0.5507	51.1250	20.4949	368.9082	4.1088
18	0.0343	0.5849	50.7824	20.4949	389.4031	4.0814
19	0.0345	0.6194	50.4376	20.4949	409.8980	4.0539
20	0.0347	0.6541	50.0904	20.4949	430.3929	4.0262
21	0.0350	0.6891	49.7407	20.4949	450.8878	3.9982
22	0.0352	0.7243	49.3886	20.4949	471.3827	3.9701
23	0.0355	0.7598	49.0339	20.4949	491.8776	3.9418
24	0.0357	0.7955	48.6767	20.4949	512.3725	3.9133
25	0.0360	0.8315	48.3168	20.4949	532.8674	3.8846
26	0.0363	0.8677	47.9542	20.4949	553.3623	3.8557
27	0.0365	0.9043	47.5888	20.4949	573.8572	3.8265
28	0.0368	0.9411	47.2207	20.4949	594.3521	3.7971
29	0.0371	0.9782	46.8496	20.4949	614.8470	3.7675
30	0.0374	1.0156	46.4756	20.4949	635.3419	3.7377
31	0.0377	1.0533	46.0985	20.4949	655.8368	3.7076
32	0.0380	1.0913	45.7183	20.4949	676.3317	3.6773
33	0.0383	1.1297	45.3350	20.4949	696.8266	3.6467
34	0.0387	1.1683	44.9483	20.4949	717.3215	3.6159
35	0.0390	1.2073	44.5583	20.4949	737.8164	3.5848
36	0.0393	1.2467	44.1649	20.4949	758.3113	3.5534
37	0.0397	1.2864	43.7679	20.4949	778.8062	3.5217
38	0.0401	1.3264	43.3673	20.4949	799.3011	3.4898
39	0.0404	1.3669	42.9630	20.4949	819.7960	3.4575
40	0.0408	1.4077	42.5548	20.4949	840.2909	3.4250
41	0.0412	1.4489	42.1427	20.4949	860.7858	3.3921
42	0.0416	1.4905	41.7265	20.4949	881.2807	3.3590

43	0.0420	1.5326	41.3061	20.4949	901.7756	3.3255
44	0.0425	1.5750	40.8814	20.4949	922.2705	3.2916
45	0.0429	1.6179	40.4522	20.4949	942.7654	3.2574
46	0.0434	1.6613	40.0184	20.4949	963.2603	3.2229
47	0.0439	1.7052	39.5799	20.4949	983.7552	3.1879
48	0.0443	1.7495	39.1364	20.4949	1004.2501	3.1526
49	0.0449	1.7944	38.6879	20.4949	1024.7450	3.1169
50	0.0454	1.8398	38.2341	20.4949	1045.2399	3.0807
51	0.0459	1.8857	37.7748	20.4949	1065.7348	3.0442
52	0.0465	1.9322	37.3100	20.4949	1086.2297	3.0072
53	0.0471	1.9792	36.8392	20.4949	1106.7246	2.9697
54	0.0477	2.0269	36.3623	20.4949	1127.2195	2.9317
55	0.0483	2.0752	35.8791	20.4949	1147.7144	2.8933
56	0.0490	2.1242	35.3893	20.4949	1168.2093	2.8543
57	0.0497	2.1739	34.8927	20.4949	1188.7042	2.8148
58	0.0504	2.2243	34.3888	20.4949	1209.1991	2.7747
59	0.0511	2.2754	33.8775	20.4949	1229.6940	2.7341
60	0.0519	2.3273	33.3584	20.4949	1250.1889	2.6928
61	0.0527	2.3801	32.8310	20.4949	1270.6838	2.6509
62	0.0536	2.4337	32.2950	20.4949	1291.1787	2.6083
63	0.0545	2.4882	31.7500	20.4949	1311.6736	2.5650
64	0.0555	2.5436	31.1954	20.4949	1332.1685	2.5210
65	0.0565	2.6001	30.6308	20.4949	1352.6634	2.4762
66	0.0575	2.6576	30.0556	20.4949	1373.1583	2.4305
67	0.0586	2.7162	29.4692	20.4949	1393.6532	2.3840
68	0.0598	2.7761	28.8709	20.4949	1414.1481	2.3365
69	0.0611	2.8372	28.2599	20.4949	1434.6430	2.2881
70	0.0625	2.8996	27.6354	20.4949	1455.1379	2.2386
71	0.0639	2.9635	26.9964	20.4949	1475.6328	2.1880
72	0.0654	3.0290	26.3420	20.4949	1496.1277	2.1362
73	0.0671	3.0961	25.6709	20.4949	1516.6226	2.0831
74	0.0689	3.1650	24.9817	20.4949	1537.1175	2.0286
75	0.0709	3.2359	24.2730	20.4949	1557.6124	1.9727
76	0.0730	3.3089	23.5430	20.4949	1578.1073	1.9150
77	0.0753	3.3842	22.7896	20.4949	1598.6022	1.8556
78	0.0779	3.4621	22.0105	20.4949	1619.0971	1.7943
79	0.0808	3.5429	21.2027	20.4949	1639.5920	1.7307
80	0.0840	3.6269	20.3629	20.4949	1660.0869	1.6647
81	0.0876	3.7145	19.4869	20.4949	1680.5818	1.5960
82	0.0917	3.8062	18.5697	20.4949	1701.0767	1.5242
83	0.0965	3.9027	17.6048	20.4949	1721.5716	1.4488
84	0.1021	4.0048	16.5838	20.4949	1742.0665	1.3693
85	0.1088	4.1136	15.4956	20.4949	1762.5614	1.2848
86	0.1171	4.2307	14.3251	20.4949	1783.0563	1.1943
87	0.1275	4.3582	13.0500	20.4949	1803.5512	1.0964
88	0.1414	4.4996	11.6359	20.4949	1824.0461	0.9887
89	0.1612	4.6607	10.0244	20.4949	1844.5410	0.8675
90	0.1926	4.8533	8.0983	20.4949	1865.0359	0.7258
91	0.2560	5.1093	5.5385	20.4949	1885.5308	0.5462
92	0.5539	5.6632	0.0000	20.4949	1906.0257	0.0000

APPENDIX E

Shoes Contact Area

Picture below shows the shoe position or contact area for Load Step 1 to 9.

Black colour is representing Shoe 1 while Red colour is Shoe 2.

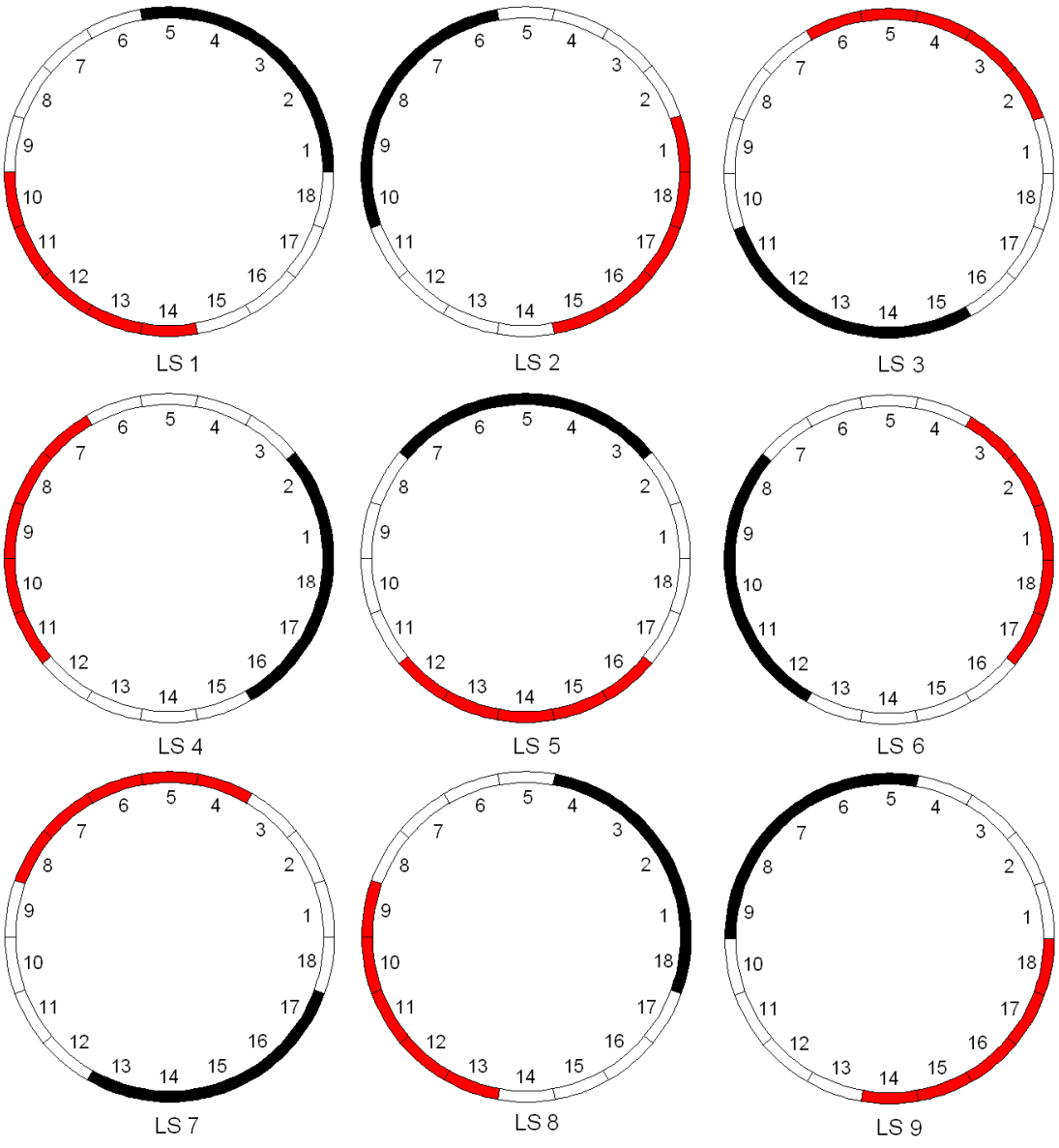

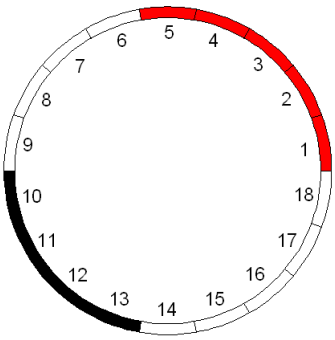

LS 10

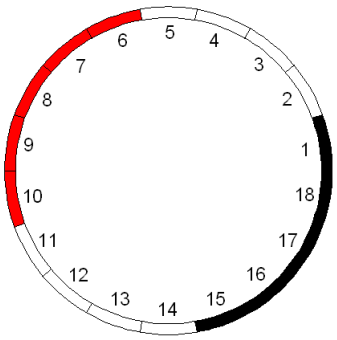

LS 11

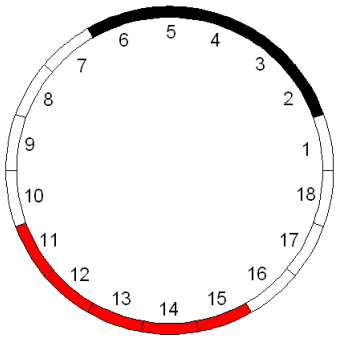

LS 12

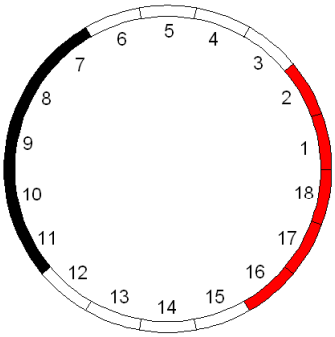

LS 13

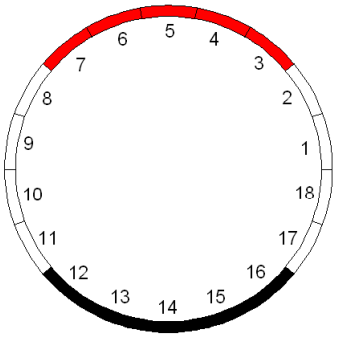

LS 14

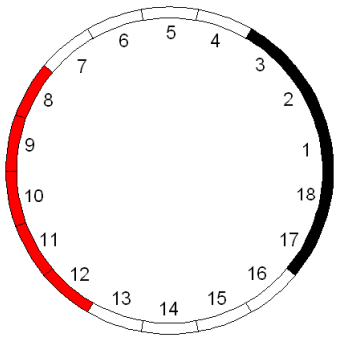

LS 15

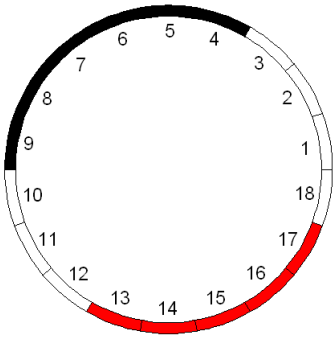

LS 16

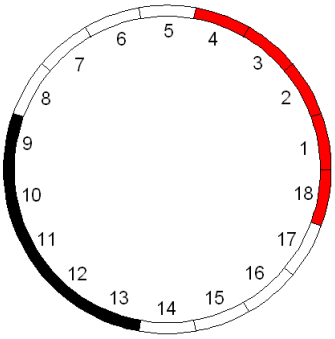

LS 17

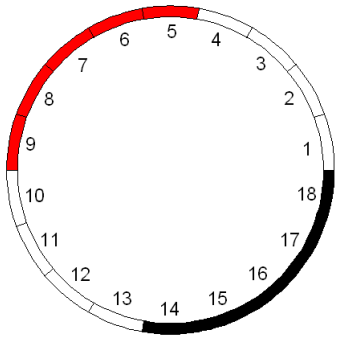

LS 18

APPENDIX F

C++ Coding program to generate ANSYS command text

```
#include <stdio.h>
#include <string.h>
#include <conio.h>
#include <math.h>

void main ()
{
  FILE *input;
  input = fopen("e:\\Coding_ANSYS_Command.txt","w");

  float v=0, u=27.778, a=-4.905, A=0.0733;
  float t_stop, d;

  float alpha=-10, teta=1.7453;
  float delta_t=0.0, accum_t=0.0;
  float w0=56.632, w1;

  float Q=20494.9;
  float q;


  t_stop = (v-u)/a;
  d = ((v*v)-(u*u))/(2*a);


  int i, j = 1;

       for (i=1;i<92;i++){
              w1 = sqrt((w0*w0)+(2*alpha*teta));
    delta_t  = (w1-w0)/alpha;

    q = ((0.5*Q)/(A*delta_t))/1000000;

    fprintf(input,"!Load Step %d\n\n",i);
              fprintf(input,"ASEL,,AREA,,ALL_AREA\n");
              fprintf(input,"CM,ALL_AREA,AREA\n");
              fprintf(input,"ASEL,,AREA,,FLUX%d\n",j);
              fprintf(input,"CM,FLUX%d,AREA\n\n",j);
              fprintf(input,"ASEL,S,AREA,,ALL_AREA\n");
              fprintf(input,"ASEL,U,AREA,,FLUX%d\n",j);
              fprintf(input,"SFA,ALL,1,CONV,51\n\n");
              fprintf(input,"ASEL,S,AREA,,FLUX%d\n\n",j);
              fprintf(input,"SFA,ALL,1,HFLUX,%fe6\n",q);
              fprintf(input,"ALLSEL,ALL\n\n");
```

```
        accum_t += delta_t;

                fprintf(input,"TIME,%f\n",accum_t);
                fprintf(input,"AUTOS,-1\n");
                fprintf(input,"NSUBST,5,,,1\n");
                fprintf(input,"KBC,1\n");
        fprintf(input,"OUTRES,BASIC,LAST\n");
        fprintf(input,"OUTPR,BASIC\n\n");
                fprintf(input,"TSRES,ERASE\n\n");
                fprintf(input,"LSWRITE,%d\n\n",i);
                fprintf(input,"ASEL,,AREA,,ALL_AREA\n");
                fprintf(input,"SFADELE,ALL_AREA,1,ALL\n\n\n");
                fprintf(input,"!***\n");

        w0=w1;
        if(w0 < 0)
          break;

        j++;
        if(j == 10){
          j = 1;
        }
    }

    getch();
}
```

APPENDIX G

Sample ANSYS command text

- **Thermal Analysis**

```
!Load Step 1                          ! Load Step No.

ASEL,,AREA,,ALL_AREA                  ! Select the area component
CM,ALL_AREA,AREA                      ! Group the areas into a component
ASEL,,AREA,,FLUX1
CM,FLUX1,AREA

ASEL,S,AREA,,ALL_AREA                 ! Select the convection area
ASEL,U,AREA,,FLUX1
SFA,ALL,1,CONV,51                     ! Define convection coefficient on area

ASEL,S,AREA,,FLUX1                    ! Select the heat flux area
SFA,ALL,1,HFLUX,4.523958e6            ! Define heat flux on area
ALLSEL,ALL

TIME,0.030902                         ! Define the time step
AUTOS,-1
NSUBST,5,,,1
KBC,1
OUTRES,BASIC,LAST
OUTPR,BASIC
TSRES,ERASE

LSWRITE,1                             ! Write to load step file no. 1

ASEL,,AREA,,ALL_AREA                  ! Select all areas
SFADELE,ALL_AREA,1,ALL                ! Delete all surface loads


!***
```

- **Structural Analysis**

```
!Load Step 1                                    ! Load step No.

LDREAD,TEMP,1,,,0,3D_Temperature.rth            ! Read result from the temperature file
LSWRITE,1                                       ! Write to load step file no. 1

!Load Step 2

LDREAD,TEMP,2,,,0,3D_Temperature.rth
LSWRITE,2

!Load Step 3

LDREAD,TEMP,3,,,0,3D_Temperature.rth
LSWRITE,3

!Load Step 4

LDREAD,TEMP,4,,,0,3D_Temperature.rth
LSWRITE,4

!Load Step 5

LDREAD,TEMP,5,,,0,3D_Temperature.rth
LSWRITE,5

!Load Step 6

LDREAD,TEMP,6,,,0,3D_Temperature.rth
LSWRITE,6

!Load Step 7

LDREAD,TEMP,7,,,0,3D_Temperature.rth
LSWRITE,7

!Load Step 8

LDREAD,TEMP,8,,,0,3D_Temperature.rth
LSWRITE,8
```

APPENDIX H

Temperature Contour

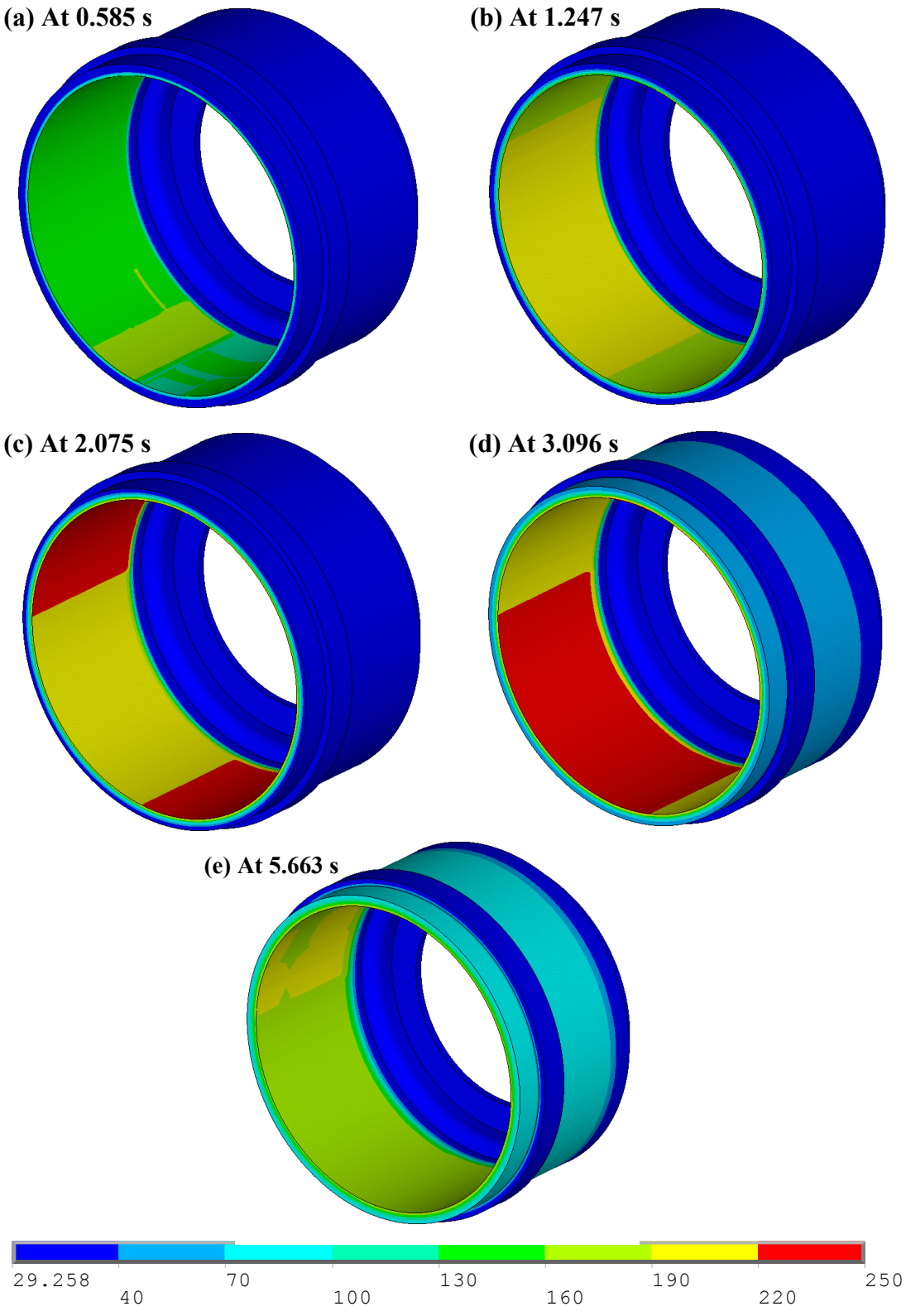

Figure H-1: Surface temperature contour for case 1- with circumferential fin drum

(a) At 0.585 s

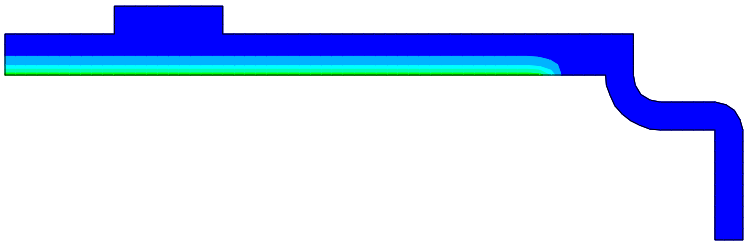

(b) At 1.247 s

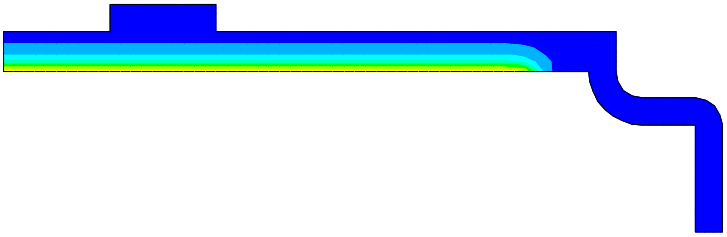

(c) At 2.075 s

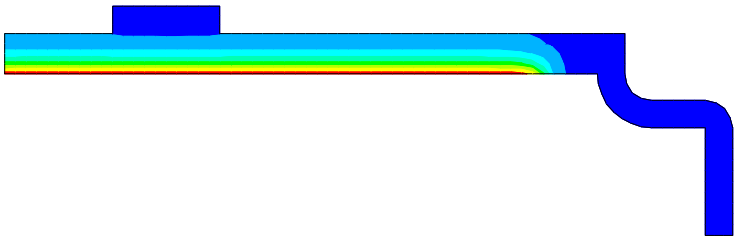

(d) At 3.096 s

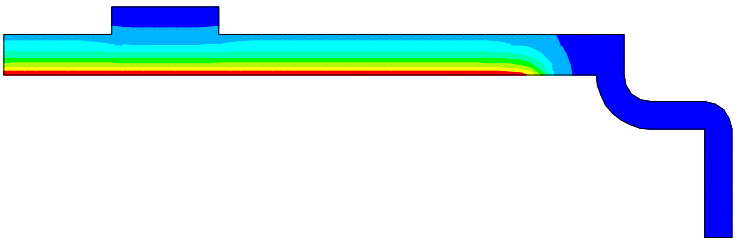

(e) At 5.633 s

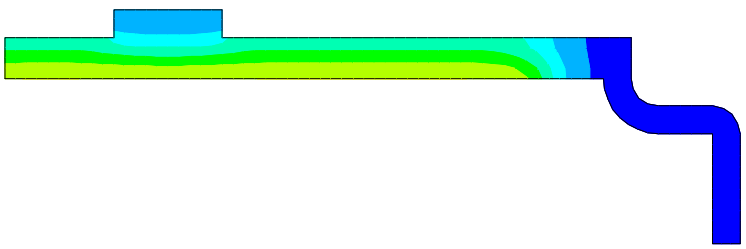

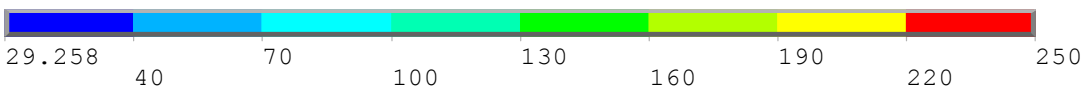

Figure H-2: Inner temperature contour for case 1 - with circumferential fin drum

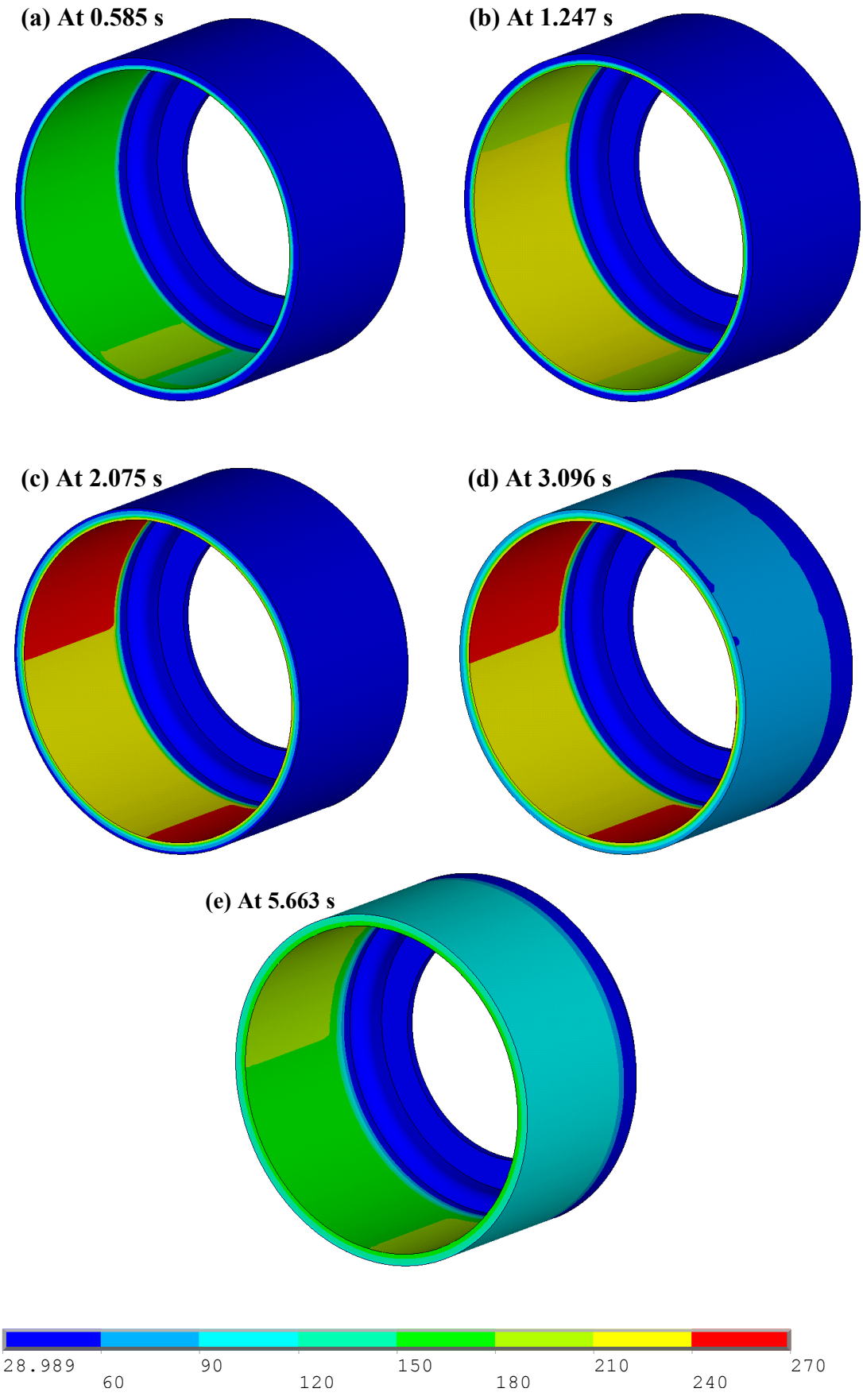

Figure H-3: Surface temperature contour for case 2 - without circumferential fin drum

(a) At 0.585 s

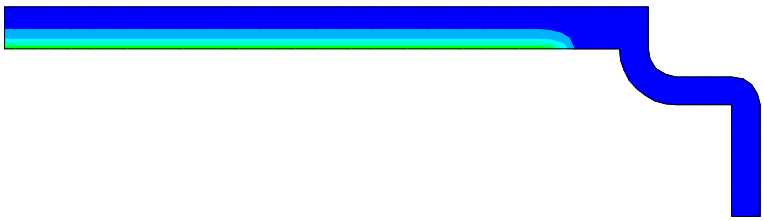

(b) At 1.247 s

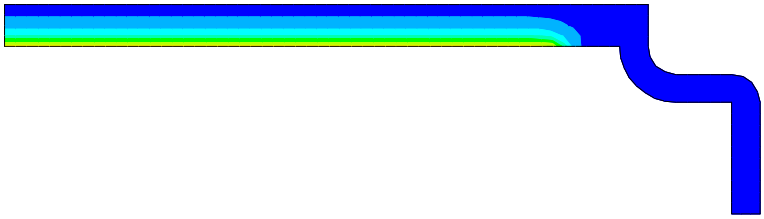

(c) At 2.075 s

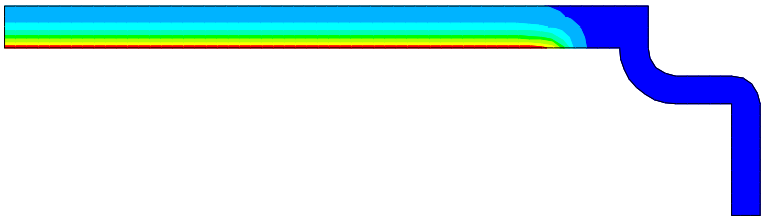

(d) At 3.096 s

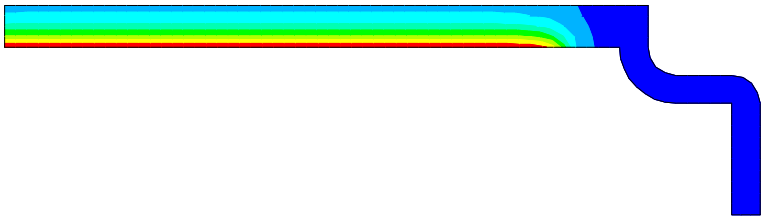

(e) At 5.633 s

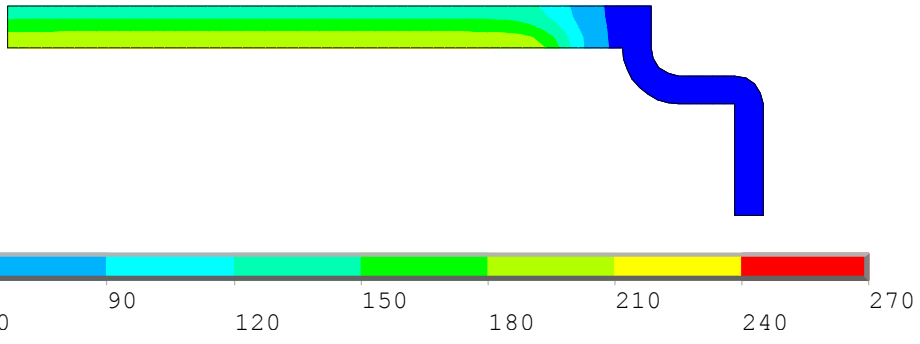

Figure H-4: Inner temperature contour for case 2 - without circumferential fin drum

APPENDIX I

Thermal Stress Contour

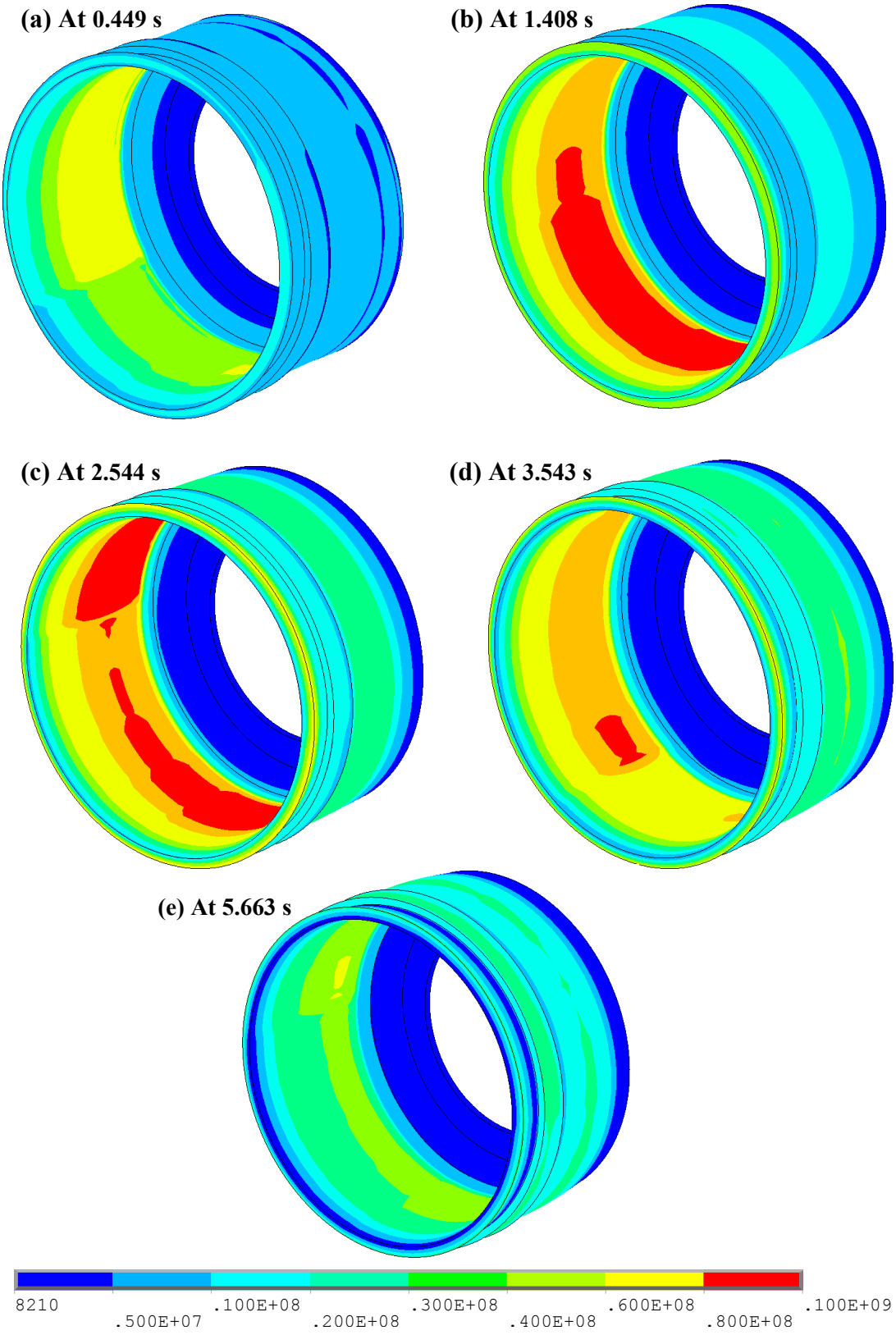

Figure I-1: Surface thermal stress contour for case 1 - with circumferential fin drum

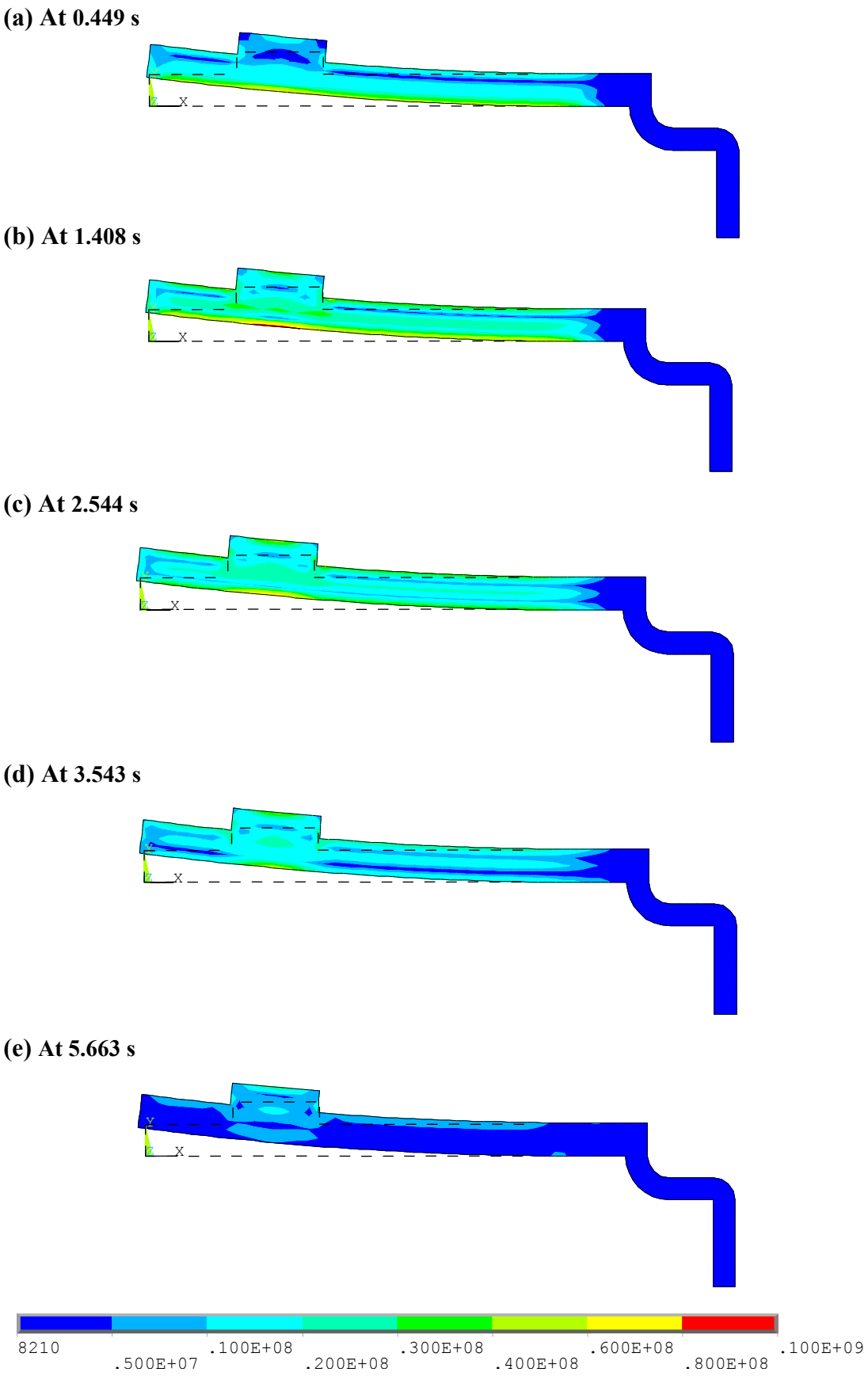

Figure I-2: Inner thermal stress contour for case 1 - with circumferential fin drum

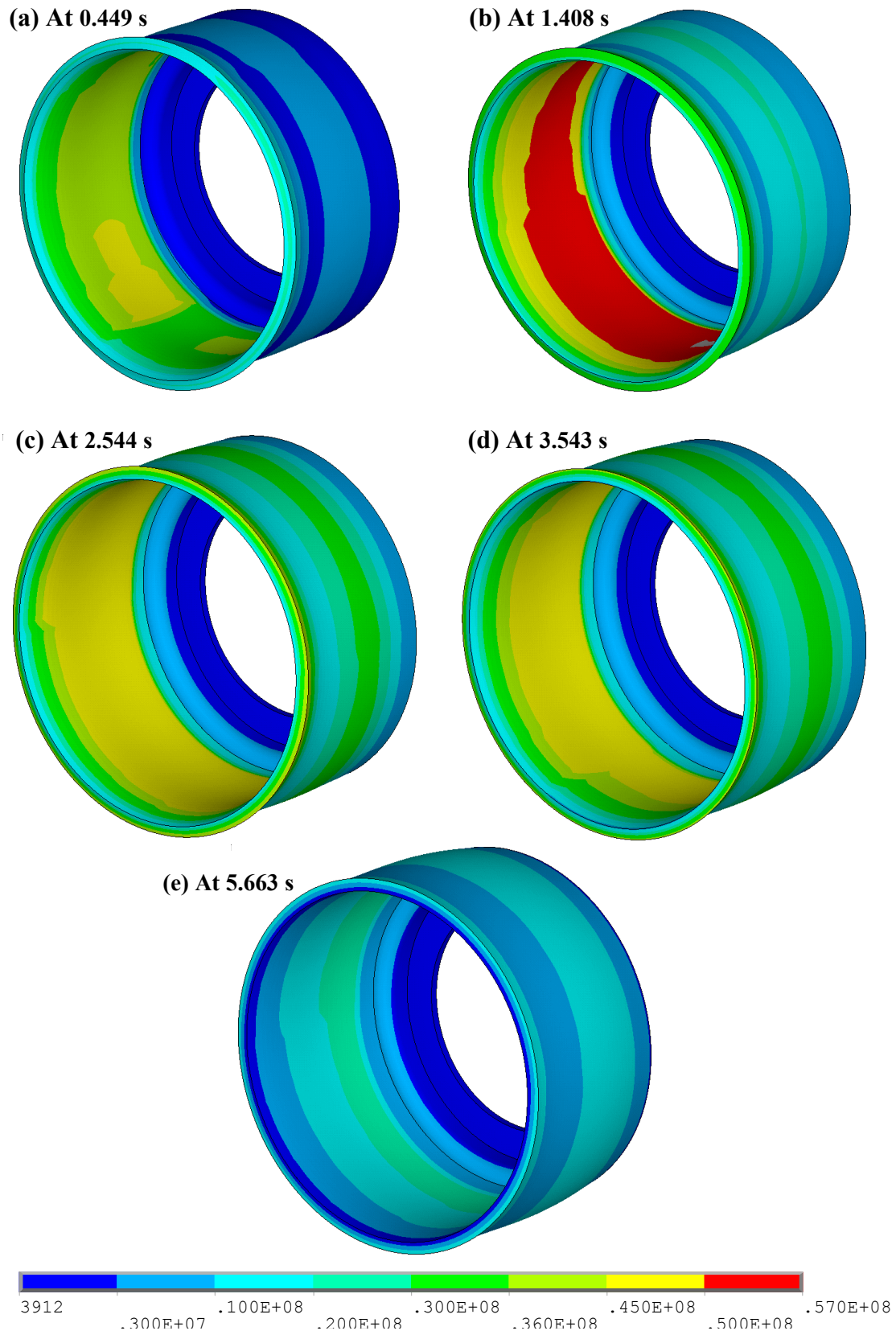

Figure I-3: Surface thermal stress contour for case 2 - without circumferential fin drum

(a) At 0.449 s

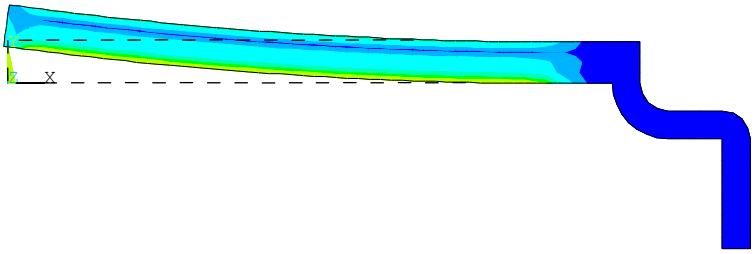

(b) At 1.408 s

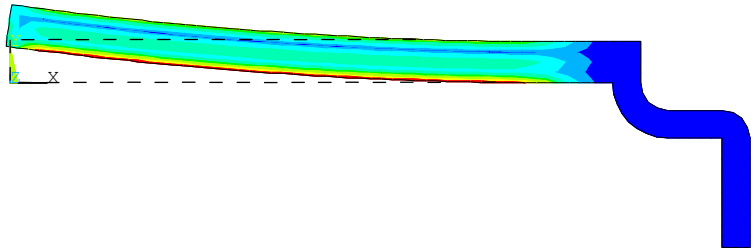

(c) At 2.544 s

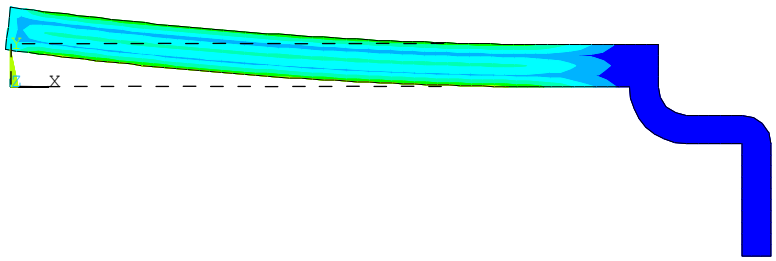

(d) At 3.543 s

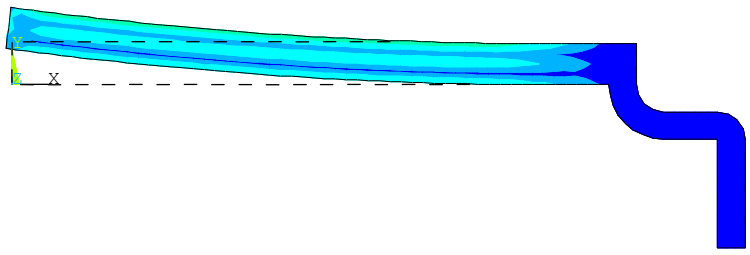

(e) At 5.663 s

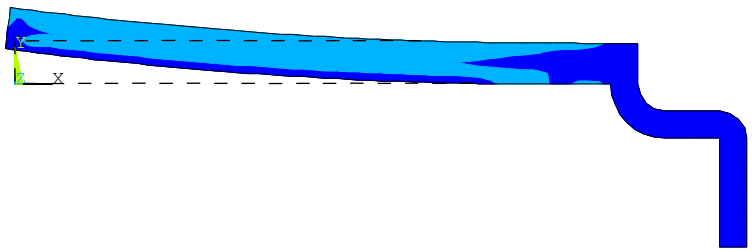

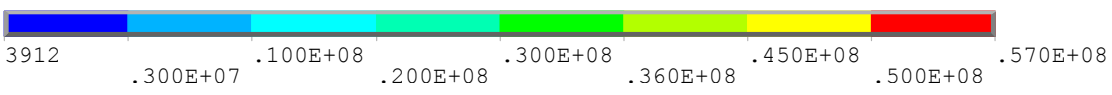

Figure I-4: Inner thermal stress contour for case 2 - without circumferential fin drum

APPENDIX J

Thermal Expansion Contour

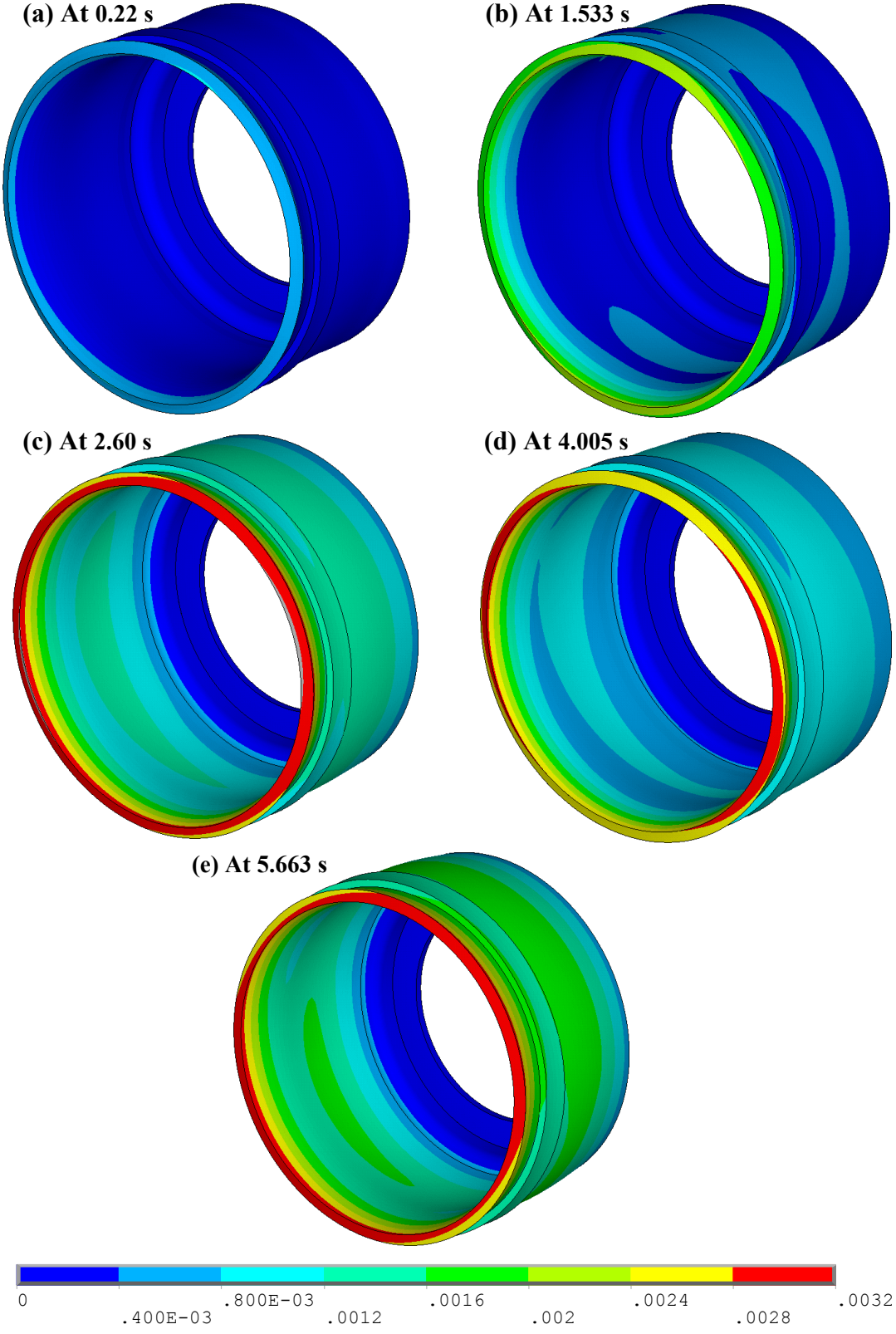

Figure J-1: Surface thermal expansion contour for case 1 - with circumferential fin drum

(a) At 0.22 s

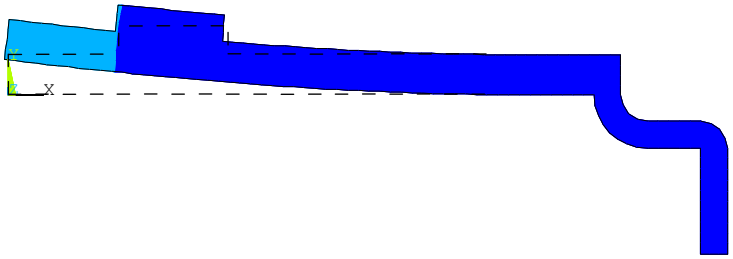

(b) At 1.533 s

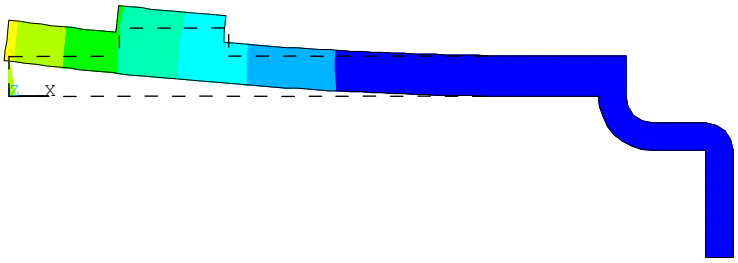

(c) At 2.60 s

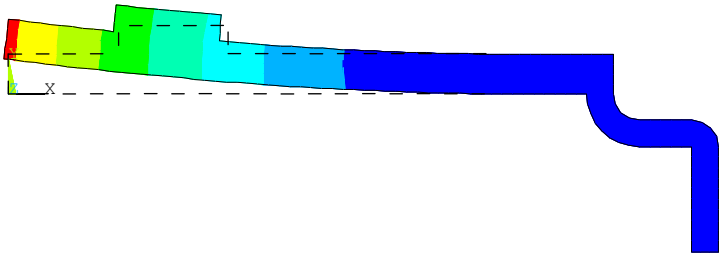

(d) At 4.005 s

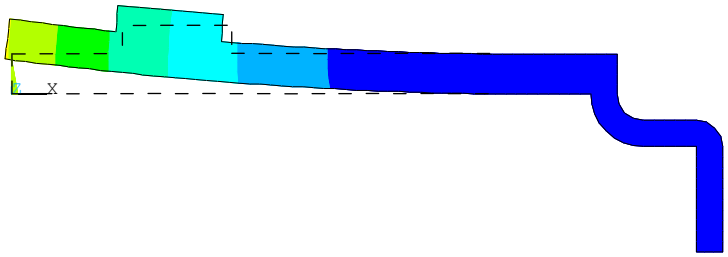

(e) At 5.663 s

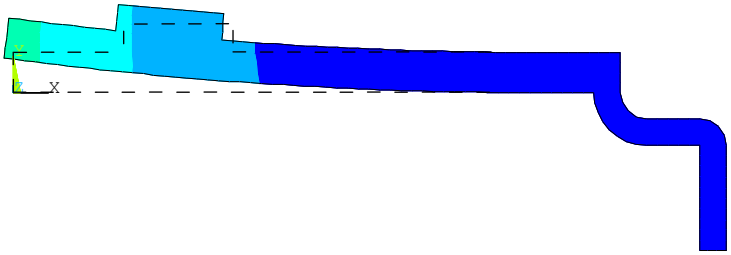

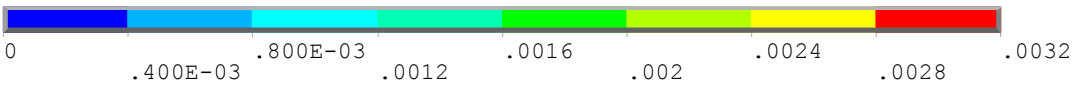

Figure J-2: Inner thermal expansion contour for case 1 - with circumferential fin drum

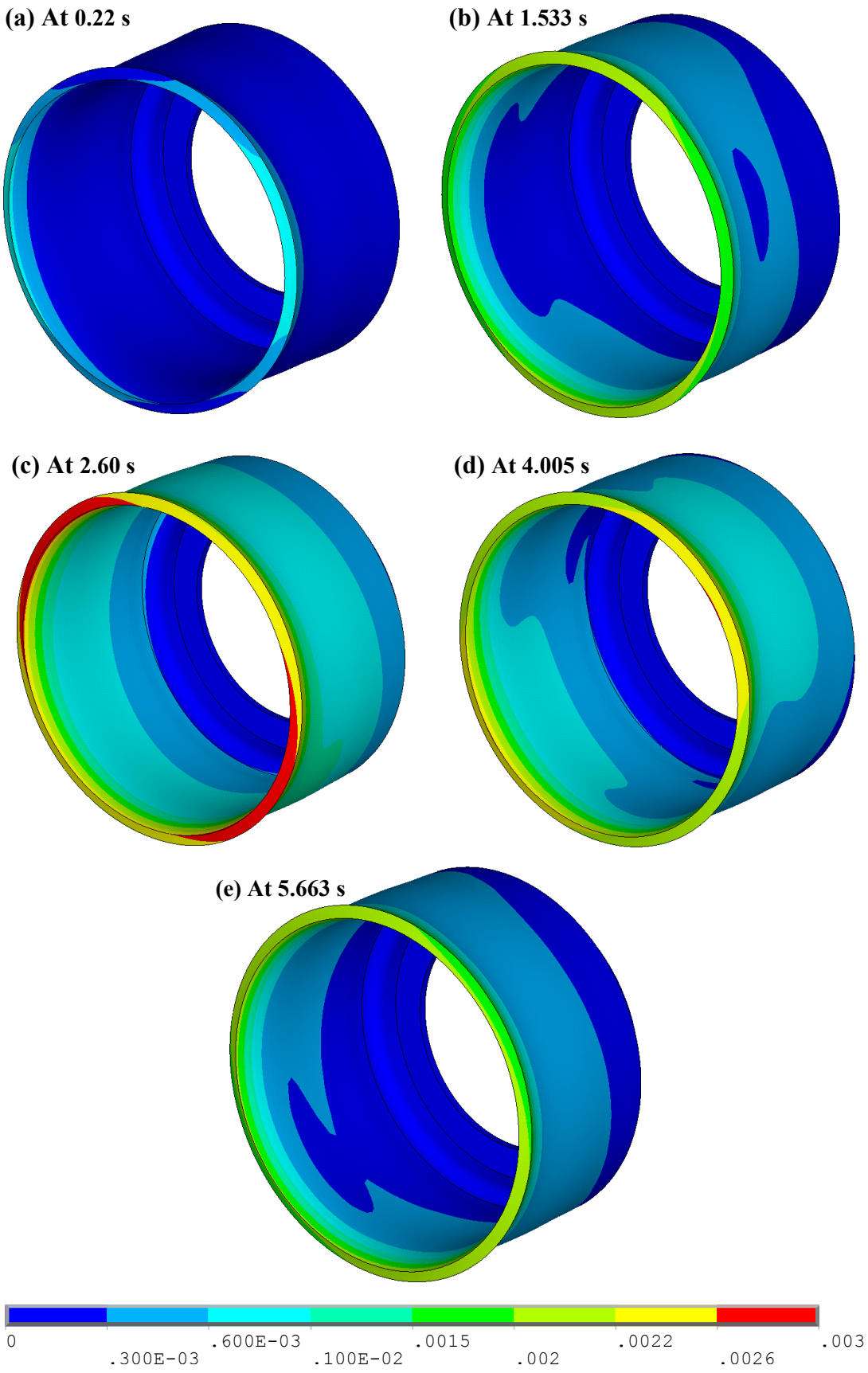

Figure J-3: Surface thermal expansion contour for case 2 - without circumferential fin drum

(a) At 0.22 s

(b) At 1.533 s

(c) At 2.60 s

(d) At 4.005 s

(e) At 5.663 s

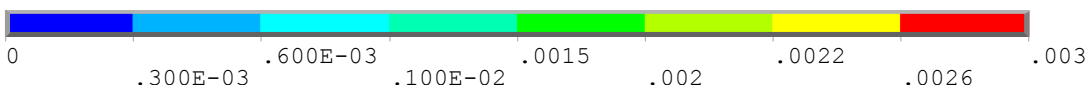

Figure J-4: Inner thermal expansion contour for case 2 - without circumferential fin drum